Marine Micropaleontology 114 (2015) 19–35

Contents lists available at ScienceDirect

Marine Micropaleontology

journal homepage: www.elsevier.com/locate/marmicro

Research paper

Genetic and morphometric evidence for parallel evolution of the *Globigerinella calida* morphotype

Agnes K.M. Weiner [a,*], Manuel F.G. Weinkauf [a], Atsushi Kurasawa [b], Kate F. Darling [c,d], Michal Kucera [a]

[a] MARUM Center for Marine Environmental Sciences, University of Bremen, Leobenerstrasse, 28359 Bremen, Germany
[b] Research and Development Center for Global Change, Japanese Agency for Marine Earth Science and Technology, Natsushima-cho 2-15, Yokosuka 237-0061, Japan
[c] School of GeoSciences, University of Edinburgh, Edinburgh EH9 3JW, UK
[d] School of Geography and GeoSciences, University of St Andrews, Fife KY16 9AL, UK

ARTICLE INFO

Article history:
Received 1 April 2014
Received in revised form 14 October 2014
Accepted 16 October 2014
Available online 25 October 2014

Keywords:
planktonic foraminifera
Globigerinella
shell morphology
shell porosity
taxonomy
parallel evolution

ABSTRACT

Molecular genetic investigations of the highly abundant extant planktonic foraminifera plexus *Globigerinella siphonifera*/*Globigerinella calida* have recently shown this group to be the genetically most diverse one within planktonic foraminifera, separating it into 12 distinct genetic types belonging to three main genetic lineages. Independently, several morphological or physiological variants have been described within the group, but the correlation between the high genetic diversity and the phenotypic variability remains unclear. In this study, we combine genetic data with morphometric analyses of shell shape and porosity of genotyped individuals of the different genetic lineages. Our morphometric measurements suggest a differentiation of three morphotypes within the plexus, two of which possess the elongated chambers described as a typical trait of *G. calida*. These two morphotypes with elongated chambers are associated with two distinct genetic lineages. The *G. calida* morphology therefore appears to have evolved twice in parallel. Unexpectedly, we show that the two morphotypes with elongated chambers can be separated from each other by characters seen in the lateral view of their shells. This implies that the taxonomy of the extant members of the genus *Globigerinella* should be revised. A comparison with the original descriptions and type specimens of members of the genus shows that two genetic types of one major lineage correspond to *G. calida*. The second group with elongated chambers is associated with a recently diverged genetic type and we propose to reinstate the name *Globigerinella radians* for this distinct form. The remaining nine of the 12 genetic types correspond to the *G. siphonifera* morphology, and in the absence of evidence for morphological differentiation, they form a paraphyletic morpho-taxon. Our results highlight the prevalence of parallelism in the evolution of shell morphology in planktonic foraminifera even at the lowest level of relatedness represented by genetic types.

1. Introduction

Molecular genetic studies of extant planktonic foraminifera continue to challenge our perception on the diversity within the group (e.g. Darling et al., 1999; de Vargas et al., 1999; de Vargas et al., 2002; Aurahs et al., 2009; Seears et al., 2012; Quillévéré et al., in press). The relatively low number of accepted morphospecies (e.g. Hemleben et al., 1989) is significantly exceeded by the number of their constituent genetic types (e.g. Darling and Wade, 2008). Since most of these genetic types cannot be differentiated morphologically, they are often referred to as "cryptic species" and their discovery usually has no impact on the taxonomy of the morphospecies. Exceptions hereto are *Neogloboquadrina incompta*, which could be separated from *Neogloboquadrina pachyderma* based on genetic data confirming the observation that the two species are characterized by different coiling directions (Darling et al., 2006) as well as *Globigerinoides elongatus* that was initially synonymized with *Globigerinoides ruber*, but recently shown to be genetically as well as morphologically distinct (Aurahs et al., 2011). Morphometric studies on *Orbulina universa*, *Globoconella inflata* and *Globorotalia truncatulinoides* revealed only slight morphological differences between the genetic types that were statistically significant, but did not allow sufficiently precise discrimination of individuals to warrant a taxonomic revision (Morard et al., 2009; Morard et al., 2011; Quillévéré et al., in press). A study on the morphospecies complex *Globigerinoides sacculifer* surprisingly revealed that also the opposite scenario can exist: a worldwide screening of all morphotypes associated with this taxon showed that this morphospecies is genetically homogenous despite high morphological variability (André et al., 2013). In this case an over-interpretation of morphological characteristics had taken place, which led to the usage of multiple morphospecies concepts that do not appear justified in the light of the

* Corresponding author. Tel.: +49 421 21865972; fax: +49 421 21865505.
E-mail address: aweiner@marum.de (A.K.M. Weiner).

http://dx.doi.org/10.1016/j.marmicro.2014.10.003

genetic evidence. These examples underline that the connection between genetic and morphologic variability in planktonic foraminifera is complex and the resolution of species delineation requires a detailed combined genetic and morphometric analysis. Here we present such combined analysis for the genetically and morphologically diverse *Globigerinella siphonifera*/*Globigerinella calida* plexus.

The genus *Globigerinella* was first described by Cushman (1927) to include individuals with near-planispirally coiled shells, globular to ovate chambers and fine rounded spines (Kennett and Srinivasan, 1983). Three extant morphospecies can be attributed to this highly diverse and abundant genus. The most abundant morphospecies is *G. siphonifera*, described as *Globigerina siphonifera* by d'Orbigny (1839), with spherical to ovate chambers and a rather tight coiling. *Globigerina aequilateralis*, described by Brady (1879), which has a very similar morphology, was later declared a junior synonym (Banner and Blow, 1960). The second most abundant morphospecies, *G. calida*, was described as *Globigerina calida* by Parker (1962). It was characterized as having trochospirally coiled evolute shells with radially elongated chambers, the final chamber separated from the previous ones and being perforated by large circular pores (Parker, 1962; Saito et al., 1981). Both species occur globally in the surface waters of the tropics, subtropics and the temperate regions (e.g. Bé, 1977; Huber et al., 1997). The third morphospecies is *Globigerinella adamsi*, which was originally described as *Hastigerina adamsi* (Banner and Blow, 1959) and is characterized by its elongated digitate chambers with pointed tips. This morphospecies is exceedingly rare. It inhabits mesopelagic waters of the Indopacific low latitude realm (Bé and Tolderlund, 1971) and was never collected for genetic analysis. All three morphospecies show a considerable level of intraspecific morphological variability. Parker (1962) was the first to describe a potential separation of *G. siphonifera* into two or even more groups based on shell size and the degree of deviation from the planispiral coiling. She assumed though that these forms represent ecophenotypic plasticity and therefore did not treat her morphotypes taxonomically. Interestingly, the existence of two groups within *G. siphonifera* was later inferred on the basis of biological differences, especially the possession of different endosymbiotic Chrysophycophyte species (Faber et al., 1988, 1989). Later studies suggested a correlation between these groups and the then known two genetic types (Huber et al., 1997), including a potential differentiation between the two types based on shell porosity. In a subsequent study, Bijma et al. (1998) observed differences in cell physiology and different isotopic compositions of the shell for these two groups. However, none of these discoveries had an impact on the taxonomy of the genus.

Genetic studies conducted on the ribosomal small subunit RNA gene (SSU rDNA) of *G. siphonifera* subsequently demonstrated that the high diversity in this morphospecies is not limited to the morphology, but is also represented at the genetic level (Huber et al., 1997; de Vargas et al., 2002; Darling and Wade, 2008; Göker et al., 2010). Most recently, Weiner et al. (2014) showed that the high sequence diversity in the group could be assigned to three major genetic lineages, which further split into 12 distinct genetic types (Fig. 1). Since no signs of hybridization are found between these genetic types, they may be considered to represent biological species (compare e.g. de Vargas et al., 2001; Darling et al., 2007). In these genetic studies, the exact status of *G. calida* remained unclear. The distinction of this morphospecies from *G. siphonifera* is difficult and in many cases the two morphospecies were lumped together for studies on fossils from the sediment (e.g. Siccha et al., 2009). The distinction is especially difficult among pre-adult individuals that are often encountered in the plankton. As a result, only a preliminary identification has been presented by genetic studies published to date, in which *G. calida* was suggested to represent one of the genetic types of the *Globigerinella* plexus (Type IV of de Vargas et al., 2002, and *G. calida* in Darling and Wade, 2008).

In order to resolve the relationship between genetic and morphologic variability in the genus, we have taken advantage of the recently developed methods for extraction of DNA from planktonic foraminifera that leave the shells intact for morphometric analysis (Morard et al., 2009; Weiner et al., 2014). Using these methods in combination with the imaging of genotyped specimens prior to DNA extraction, we have amassed a dataset of morphological measurements from 181 individual specimens identified by several researchers as *G. siphonifera* and *G. calida*, sampled within various regions of the world ocean. All of the specimens were genetically analyzed and could be assigned to one of the delineated genetic types. We combined measurements of shell morphology based on scanning electron microscopic as well as light

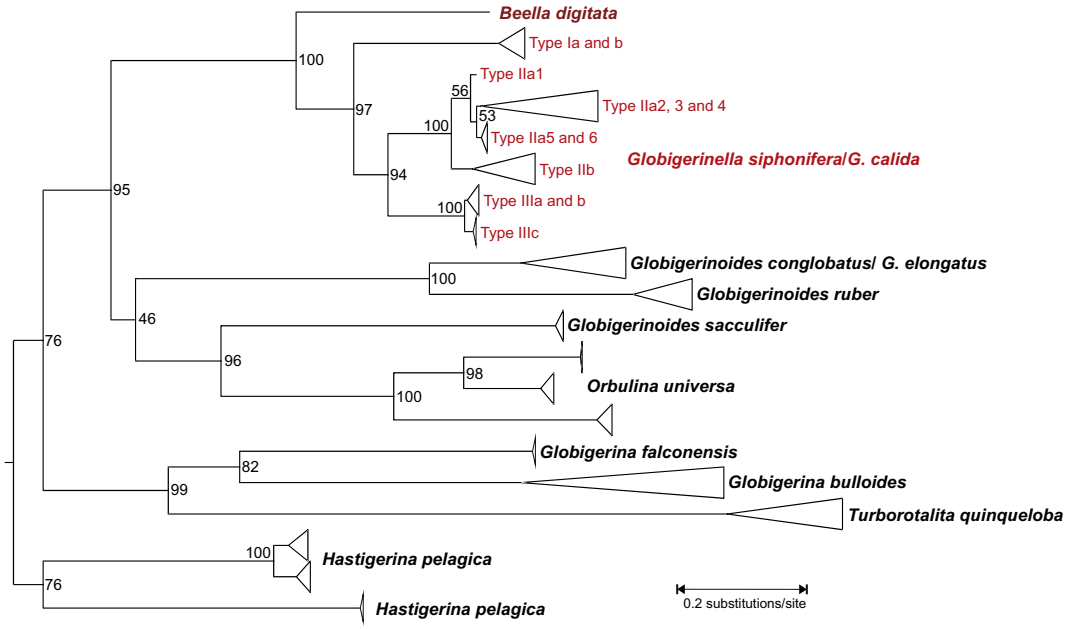

Fig. 1. Maximum likelihood phylogenetic tree of the spinose planktonic foraminifera. Phylogenetic relationships among the spinose planktonic foraminifera showing the monophyletic status of *Globigerinella* and its affinity with the sister taxon *Beella digitata* and highlighting its high genetic diversity. The tree as well as the bootstrap values are based on a MAFFT (Katoh and Standley, 2013) alignment of SSU rDNA sequences and were calculated using RAxML (Stamatakis, 2006) via the CIPRES gateway (Miller et al., 2010). Sequence diversity within morphospecies has been collapsed, except for *G. siphonifera*/*G. calida* where only terminal branches are collapsed.

microscopic images with measurements of porosity and pore size. As a result, we were able to resolve the identity of *G. calida* and revise the taxonomic concept of the *G. siphonifera*/*G. calida* plexus.

2. Material and methods

2.1. Sampling, imaging and genetic analysis

In this study, images of 181 *Globigerinella siphonifera* and *Globigerinella calida* individuals were analyzed for comparisons of shell morphology with genetic identity. All of the individuals included yielded DNA sequences that could be used to assign them to one of the 12 lineages described by Weiner et al. (2014). The specimens were collected by stratified plankton tows during 13 expeditions between 2006 and 2013 (Fig. 2, Table S1). The foraminifera were separated from the rest of the plankton, taxonomically identified using stereomicroscopes and in most cases digitally photographed directly on board. Living specimens still containing cytoplasm were prepared for DNA extraction. Methods for genetic analysis and the sequence data of most individuals were presented in Weiner et al. (2014). Specifically for this study we genetically characterized 44 additional specimens from a transit through the South Pacific on board RV SONNE (SO226-3, Kucera and Cruise Participants, 2013). These new samples represent topotypic material for the species concept of *G. calida* as developed by Parker (1962). They were obtained by stratified tows using a multiple closing net with a mesh size of 100 μm. Foraminifera were isolated from the plankton residues, cleaned, dried and frozen on cardboard slides until further processing in the lab. The guanidine method, which allows preservation of the shell, was used for DNA extraction (e.g. Morard et al., 2009). Light microscopic images showing the standard taxonomic umbilical view were taken in the lab prior to DNA extraction and all specimens have been assigned to either *G. siphonifera* or *G. calida* by the collector, following the current taxonomy as presented e.g. in Hemleben et al. (1989). Polymerase chain reaction (PCR) was used to amplify a ~600 bp large fragment of the 3′end of the small subunit ribosomal RNA gene (SSU rDNA) using the GoTaq® G2 Hot Start polymerase (Promega) and two different primer pairs as indicated in Table S1. PCR products were purified using the QIAquick® PCR Purification Kit (Qiagen) and afterwards sequenced directly by an external service provider (Agowa, Berlin). Sequence chromatograms were checked manually for ambiguous reads and corrected where possible. Sequences of all 44 individuals were submitted to GenBank (http://www.ncbi.nlm.nih.gov/; Accession nos.: KJ202213–KJ202256). Shells that could be recovered after DNA extraction were imaged by scanning electron microscopy (SEM) from spiral/umbilical and lateral view and higher magnification close-ups of chamber wall surface were taken. In total, 37 individuals from the South Pacific yielded images that could be used for morphometric analysis.

2.2. ML tree inference and bootstrapping

In order to represent the phylogenetic position of *G. siphonifera*/*G. calida* in relation to the rest of the spinose planktonic foraminifera, sequences of 11 morphospecies were included in an automated alignment

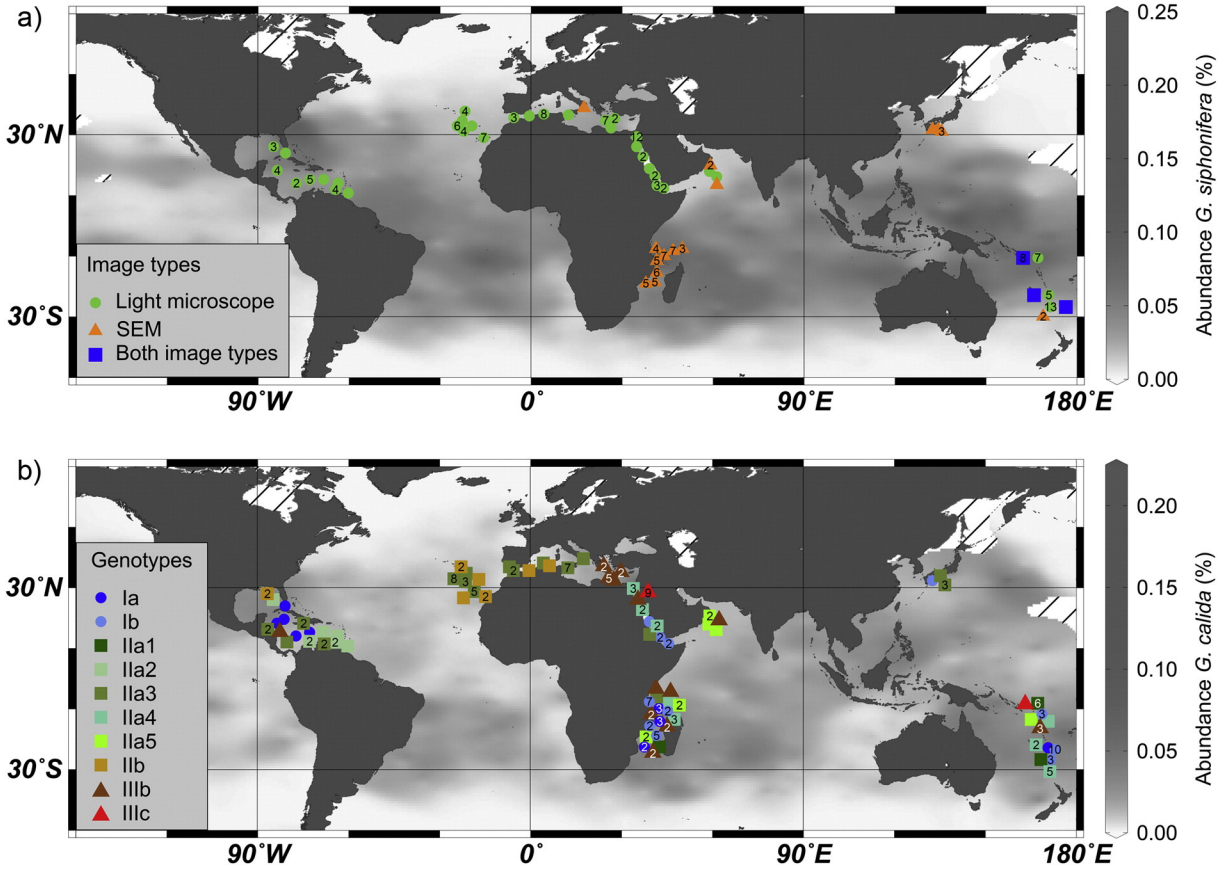

Fig. 2. Geographic locations of sampled individuals. a) Sampling locations of all individuals used in the morpho-genetic comparison in this study. Different symbols indicate where only light microscopic images, only SEM images or both were available, depending on the sampling method applied. Numbers within the symbols denote number of individuals from one sampling location. Gray shading indicates the relative abundance of *Globigerinella siphonifera* as it is found in planktonic foraminiferal assemblages from surface sediments interpolated from data in the MARGO database by Ocean Data View (Schlitzer, 2011). Diagonal lines indicate areas where no data are available. b) The genetic identity of the analyzed individuals. Symbols indicate different genetic types, following the classification by Weiner et al. (2014). Numbers within the symbols denote number of individuals from one sampling location belonging to the same genetic type. Gray shading indicates the relative abundance of *Globigerinella calida* as it is found in planktonic foraminiferal assemblages from surface sediments interpolated from data in the MARGO database by Ocean Data View. Diagonal lines indicate areas where no data are available.

using the online version of MAFFT v. 7 (File S1, Katoh and Standley, 2013) as it is available on the CIPRES gateway (Miller et al., 2010), under default settings. This alignment was then used without further manipulation or filtering for tree inference under the maximum likelihood (ML) criterion with RAxML-HPC2 v. 7.6.3 (Stamatakis, 2006) via the CIPRES Gateway. Branch support was established with the fast implementation (Stamatakis et al., 2008, option -x) of nonparametric bootstrapping (BS; Felsenstein, 1985). The number of necessary replicates was determined by automatic bootstopping with the majority-rule tree based criterion (option -#autoMRE). The per-site rate approximation model (Stamatakis, 2006) was used for the fast BS phase followed by a slow final model optimization under the general time reversible model allowing for between-site variation modeled via a gamma distribution (GTR + Γ; option -m GTRCAT). Run parameters were set to infer in one run the best-known ML tree and perform a full BS analysis (option –f a).

2.3. Measurements of shell morphology and porosity

SEM images suitable for morphometric analysis were obtained from a total of 63 specimens of the *G. siphonifera*/*G. calida* plexus in lateral and umbilical/spiral view to quantify the main morphological features of the shell which have been used to differentiate morphospecies in the plexus. The traits have been quantified as distances and landmark positions (Fig. 3) extracted from the images in R v. 3.0.1 (R Development Core Team, 2011). In lateral view these measurements include the height h_{total} of the specimen, the elongation of the last chamber (E_l), the deviation of the last whorl from the planispiral plane (expressed as angle α), and the extent to which the first chamber of the last whorl covers the aperture (PS). In umbilical/spiral view values comprise the elongation of the last chamber (E_L), the mean elongation of all chambers in the last whorl (E) and the number of chambers in the last whorl expressed as mean angle γ between successive chamber axes. To avoid the effect of unusual terminal morphologies, in Kummerform-specimens, the penultimate chamber was treated as the last chamber. Damaged specimens with fewer than three consecutive chambers in the last whorl preserved were excluded from the analysis (15 individuals). The data acquisition and parameter calculation was replicated, and the values used in the following represent the mean of the two replications to minimize subjectivity during data extraction.

To evaluate the degree of morphological separation obtained on the basis of exactly positioned clean specimens on SEM images, for practical application in the field, we subsequently tested the approach on 128 light-microscopic images of imperfectly oriented specimens in umbilical/spiral view. In these images we extracted 13 landmark points each (Fig. 3) to calculate the elongations E_L and E on the basis of the last three chambers, as well as the mean angle γ.

Porosity measurements were obtained using SEM images with a magnification of 4000 of the surfaces of the last chamber of 66 specimens. The images were treated for contrast enhancement and where necessary, pores were manually blackened to enable automatic measurements. The maximum Feret diameter (d) and centroid coordinates of each pore were then extracted from black and white threshold images in FIJI v. 1.47q (Schindelin et al., 2012). These values were then used to calculate porosity as a fraction of the pore area relative to the shell surface area (Fig. 3). This approach yields reliable results as long as pores can be expected not to be significantly oval in first approximation. The maximum pore diameter, in contrast to the directly measured pore area, is invariant to the orientation of the pore, so that the curvature of the shell does not influence the results by distorting the pores in areas which are not perfectly perpendicular to the plane of view. In this study, we decided not to break the shells to measure the pores

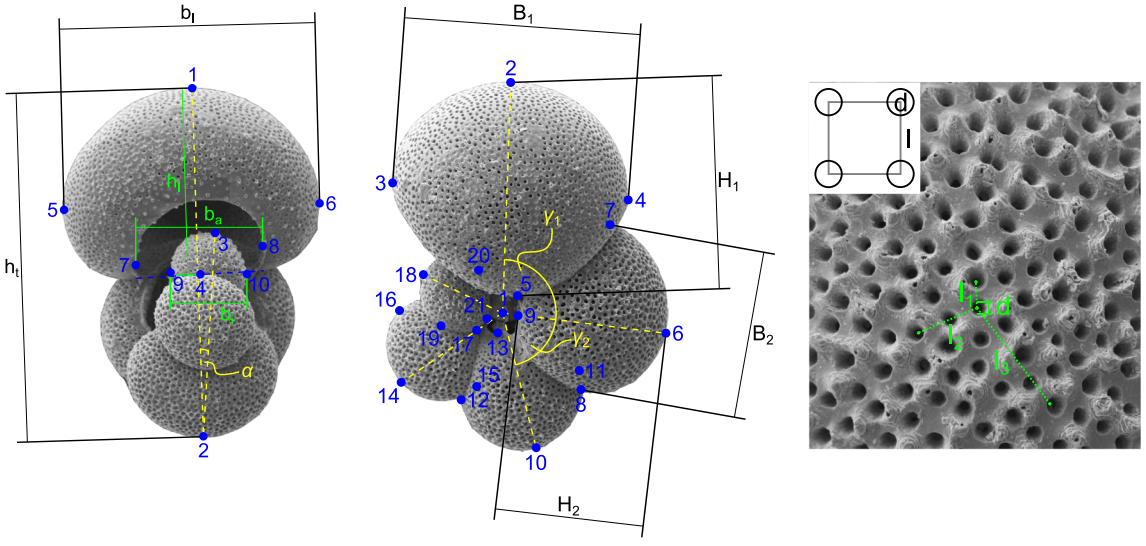

$$h_{total} = \mathrm{h_t}\ [\mu\mathrm{m}] \qquad E = \frac{\sum_{i=1}^{n} \frac{\mathrm{H}_i}{\mathrm{B}_i}}{n} \qquad \gamma = \frac{\sum_{i=1}^{n-1} \gamma_i}{n-1} \qquad \bar{d} = \frac{\sum_{i=1}^{n} d}{n} \qquad P = \frac{\frac{\pi}{4} \times \bar{d}^2}{\bar{l}^2}$$

$$\alpha = \angle 123 \qquad E_L = \frac{\mathrm{H_1}}{\mathrm{B_1}} \qquad \bar{l} = \frac{\sum_{i=1}^{n} l_{\min}}{n}$$

$$E_l = \frac{\mathrm{h_l}}{\mathrm{b_l}}$$

$$PS = \mathrm{b_i} \in \mathrm{b_a}\ [\%]$$

Fig. 3. Morphometric measurements conducted on images of *Globigerinella siphonifera*/*G. calida* individuals. Schematic representation of the measurements of shell characteristics and pore size and porosity derived from SEM images, including equations for the calculation of the derived, size-invariant parameters. Blue points represent landmarks, whose coordinates were extracted from the images. Black and green lines show distances used for the calculation of morphological parameters, which were calculated on the basis of the landmarks. Yellow dashed lines are auxiliary lines for the visualization of calculated angles. Distances H_i and B_i, and angles γ_i are only shown exemplarily on the last two chambers in umbilical view. Points 1–13 in umbilical view were also extracted from light microscopic images. (For interpretation of the references to color in this figure legend, the reader is referred to the web version of this article.)

from the inside, like Huber et al. (1997). As a result, our values are likely to overestimate pore size by a small amount, especially in large and thick shells.

In order to determine shell porosity, we calculated the distance of each pore to every other pore based on the obtained centroid coordinates in R v. 3.0.1 and then identified the nearest neighbor to each pore. The mean distance l of all nearest-neighbor-pair-distances of the specimen was then assumed to be a good approximation of the mean pore distances in that specimen. Assuming a regular pore distribution with one pore at each corner of a square with edge length l, we could then approximate the mean porosity P of the specimen ($P = (\pi / 4 \times d^2) / l^2$). Even if the real pore distribution deviates from this expectation, the fact that we treat all specimens alike, leads to mutually comparable results. In 40 specimens we have taken two SEM images from the same individual, which we could use to test the reproducibility of our results using a paired t-test.

2.4. Statistical analysis of morphometric measurements

All statistical analyses were performed in R v. 3.0.1. We used principal component analysis (PCA, Hotelling, 1933) to evaluate the continuity of the morphospace in the *G. siphonifera*/*G. calida* plexus on the basis of the morphological parameters (excluding porosity) obtained from the SEM images, without a priori assumption on their attribution to genetic types. During that step we excluded the parameter h_{total} from the analysis, because shell height of specimens from the plankton is a function of their age and does not represent the final size at which reproduction would occur. Next, we explored to what degree specimens of distinct genetic lineages can be distinguished from the rest of the plexus by performing linear discriminant analyses/canonical variate analyses (LDA/CVA, Fisher, 1936) in the R-package MASS v. 7.3-26 (Venables and Ripley, 2002). We then repeated the same steps on the data obtained from light microscopic images.

The porosity data were tested for the influence of genetic type and sampling location and their interaction term on porosity and pore size of specimens. To that end the non-parametric Scheirer–Ray–Hare test (Scheirer et al., 1976) was applied. For all significant factors, pairwise comparisons were performed using a Mann–Whitney U test (Mann and Whitney, 1947), during which the p-values were corrected after Benjamini and Hochberg (1995). To test for a relationship between pore size/porosity and shell size (approximated via shell height, h_t), we performed a Kendall–Theil robust line fitting (Kendall, 1938; Theil, 1950; Sen, 1968) implemented in R, using the equations from Helsel and Hirsch (2002) and Conover (1980). For specimens with two SEM images of the same individual, we used the one which provided a larger dataset (i.e. more pore measurements) for the analysis.

3. Results

Of the 382 genetically analyzed *Globigerinella* specimens (Weiner et al. (2014) and new data from South Pacific combined), 62 were labeled upon collection as *G. calida*. In this respect, the subset used for morphometric analysis is representative, containing 42 specimens out of 181 in total originally labeled as *G. calida*. As a first step, we investigated, whether the usage of the species name *G. calida*, as determined by traditional taxonomy during the initial collection, correlated with any of the genetic types. In fact, the comparison of the taxonomic labels and genetic identification reveals that the frequency of usage of *G. calida* varies significantly among the genetic lineages and genetic types (Fig. 4). Although there is no single genetic type which is associated exclusively with specimens labeled as *G. calida*, this name has been used more frequently for specimens in lineages I and III (Fig. 4).

Next, we ventured to resolve the correlation of genetic and morphological variability in the *G. siphonifera*/*G. calida* plexus. To this end, we first explored morphological differences among all analyzed specimens and determined how these relate to the genetic types found within this

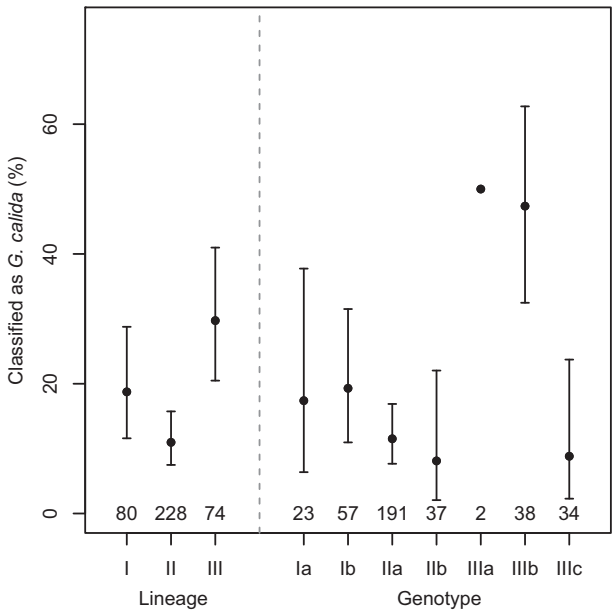

Fig. 4. Percentages of individuals classified as *Globigerinella calida*. Percentages of individuals in each genetic lineage/genetic type (following the classification by Weiner et al. (2014)) of *Globigerinella* that were classified upon collection as *G. calida*. The dataset includes all 382 individuals that were genetically analyzed, independent of the existence of morphometric measurements. Vertical bars represent 95% binomial confidence intervals after Agresti and Coull (1998). Total number of trials n is given at the bottom of the graph. Most individuals classified upon collection as *G. calida* belong to either lineage I or III.

group. The high number of SEM and light-microscopic images allowed a morphometric analysis of representatives of almost every genetic type from various parts of the world ocean (Figs. 2, 5, Table S2). Most genetic types had sufficiently well preserved shells following DNA extraction to obtain representative SEM images, apart from Types IIa2, IIa6, IIb and IIIa. However, it was possible to include Types IIa2 and IIb in the morphometric analyses using their light-microscopic images, but those of IIa6 and IIIa proved too poor to be useful.

A PCA of the morphometric measurements carried out on SEM images (Fig. 3, Table S2) revealed a significant size-independent variation in morphology of the individuals belonging to the *G. siphonifera*/*G. calida* plexus (Fig. 6). The mapping of the genetic identity onto the morphospace reveals that three of the analyzed genetic types are associated with a morphology that is distinct from the rest of the plexus. The genetic Types Ia and IIIb/c appear to be separated from the rest of the genetic types chiefly by higher chamber elongation (E_l, E_L, Fig. 6). This separation is supported by the LDA, which confirms a statistically significant difference in the multivariate means between the groups ($p < 0.001$) and reveals that based on the same set of morphological measurements, 97% of the specimens can be correctly classified by the discriminant function (Fig. 7a). Furthermore, these three types can not only be separated from the rest, they also show morphologic differences when being compared with each other. Specimens of Type Ia are characterized by the highest values for chamber elongation in spiral/umbilical view (E and E_L), while members of lineage III are marked by highest values for angle α, which describes the deviation of growth from the planispiral plane (Fig. 6). This differentiation is also supported by the LDA ($p = 0.004$), and allows a correct classification of 95% of the specimens (Fig. 7b).

A CVA with the remainder of genetic types (Ib, IIa1, IIa3–5) shows low correct classification rates (73%) and a general distribution of all genetic types over the whole morphospace, indicating that no distinct morphotypes can be separated within this group (Fig. S1).

Having established the existence of three groups of genetic types that are morphologically distinct from each other, we attempted to

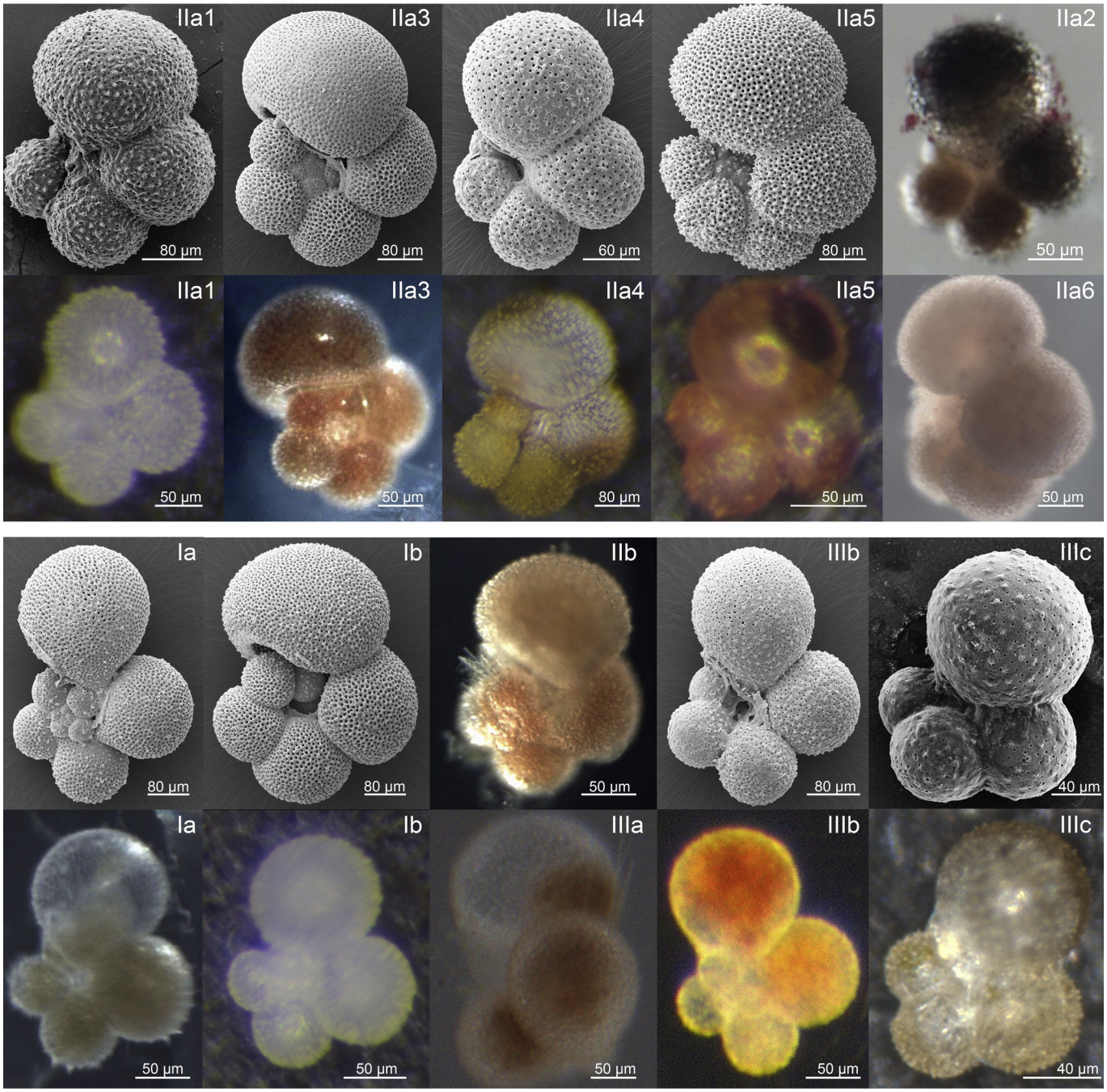

Fig. 5. Images of representative specimens of the genetic types of *Globigerinella* sp. SEM images and light microscopic images of representative individuals belonging to the different genetic types within the *G. siphonifera*/*G. calida* plexus. No SEM images are available for specimens representing Types IIa2, IIa6, IIb and IIIa. The exact sampling location of each specimen is shown in Table S1. The light microscopic images are taken immediately after sampling of living specimens.

determine whether or not these groups correspond to any of the existing morphological species concepts. To this end, we extracted images of type specimens from the literature, including original illustrations and designated types. This included the original illustrations of *Globigerina radians* by Egger (1893), *Globigerina siphonifera* by d'Orbigny (1839), its lectotype by Banner and Blow (1960) and the holotype of *Globigerina calida* by Parker (1962). The same morphological parameters have been extracted from these images as from the genotyped individuals and based on these data the specimens were projected onto the plane of the first two principal component axes (Fig. 6). This analysis reveals that the holotype of *G. calida* shows the highest similarity in morphology with the genetic Types IIIb/c. The original illustration of *G. radians* shows a specimen with highly elongated chambers and a small value of α as is characteristic for individuals of the genetic Type Ia. The rest of the genetic types clusters around the lectotype specimen of *G. siphonifera*.

In order to determine to what degree the morphological separation is possible without the time-consuming SEM imaging, we subsequently analyzed light microscopic images of 128 genotyped individuals (Table S2). Since it is not possible to take images of the lateral view without fixing the specimens, only pictures from the umbilical/spiral side were available. Consequently, the number of morphological variables was limited and characters like the angle α, that proved important for the separation into morphological groups, could not be measured. The PCA analysis of the measurements on the light microscopic images revealed that specimens belonging to Types Ia, IIIb and IIIc occupy a

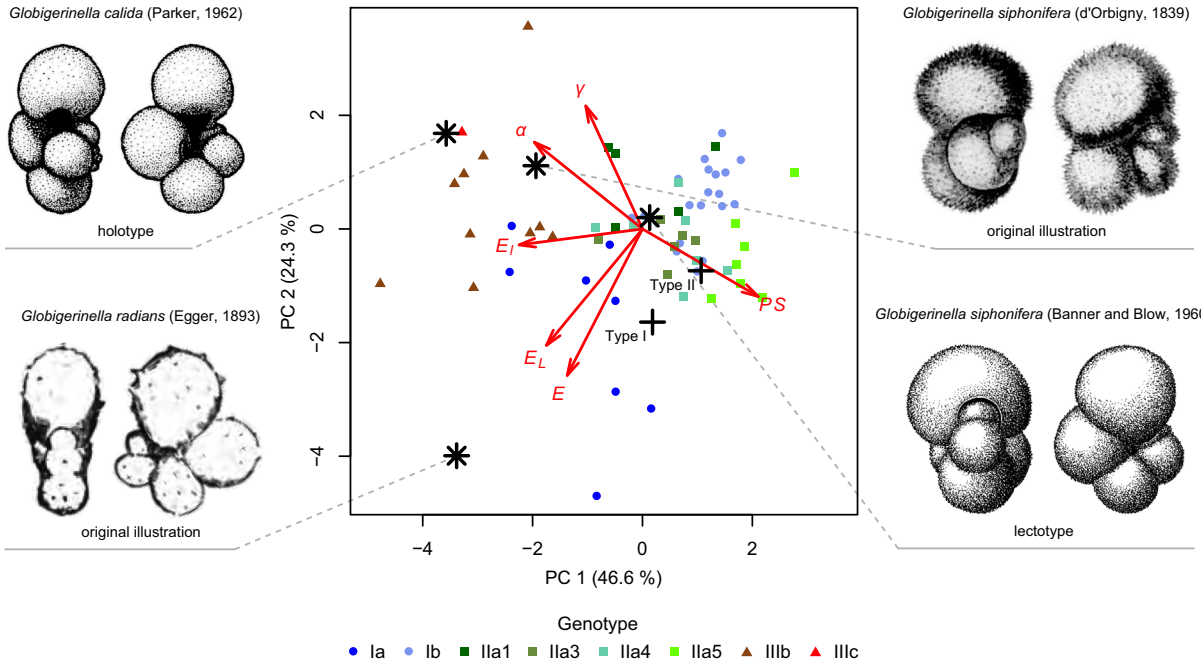

Fig. 6. PCA biplot of *Globigerinella siphonifera*/*G. calida* individuals from SEM images with projected position of type specimens. Principal component analysis (PCA) of six size-invariant morphological characters of the *G. siphonifera*/*G. calida* plexus obtained from SEM images as described in Fig. 3. The plane of the first two principle components explains 70.9% of the total variance. The projected position of type specimens (measurements obtained from the drawings shown on the side of the graph) are indicated as black stars. The type specimen of *Globigerinella adamsi* plots far outside the plot, because of the extreme elongation of the chambers and is thus not shown. The position of the extant Types I and II as described in Huber et al. (1997, Fig. 7) are projected as black crosses. Their Type I plots closer to *G. radians*, while their Type II is akin to *G. siphonifera*.

smaller portion of the total morphospace, but show a strong overlap with the rest of the genetic types (Fig. 8a). A separation between Types Ia and IIIb/c, is not apparent in this analysis. The morphological trait responsible for the position of types Ia and IIIb/c in the upper left part of the morphospace is the elongation of the chambers (mainly the last chamber), whereas the number of chambers in the last whorl proves to be variable, but not related to a certain genetic type. This finding supports the results of the SEM analyses and confirms that chamber elongation is the most important distinction factor. In comparison to the analysis based on SEM images, a differentiation into morphological groups solely on the basis of light microscopic images proves to be difficult and the LDA only classifies 78% of individuals correctly, although the difference between the groups remains highly significant at $p < 0.001$ (Fig. 8b). As implied by the results of the PCA, a further separation between genetic Types Ia and IIIb/c by an LDA is not possible ($p = 0.738$).

The final characteristic of the calcite shell that might be useful for a differentiation of genetic types is the porosity (Table S3). In an earlier study Huber et al. (1997) detected differences in porosity for individuals they attributed to two different morphological types of *G. siphonifera*, that were first described by Faber et al. (1988, 1989). Therefore, we analyzed high magnification SEM images of shell wall surface of the last chamber of 66 specimens that had also been used for the morphometric analysis (Fig. 3). A median of 104 pores were

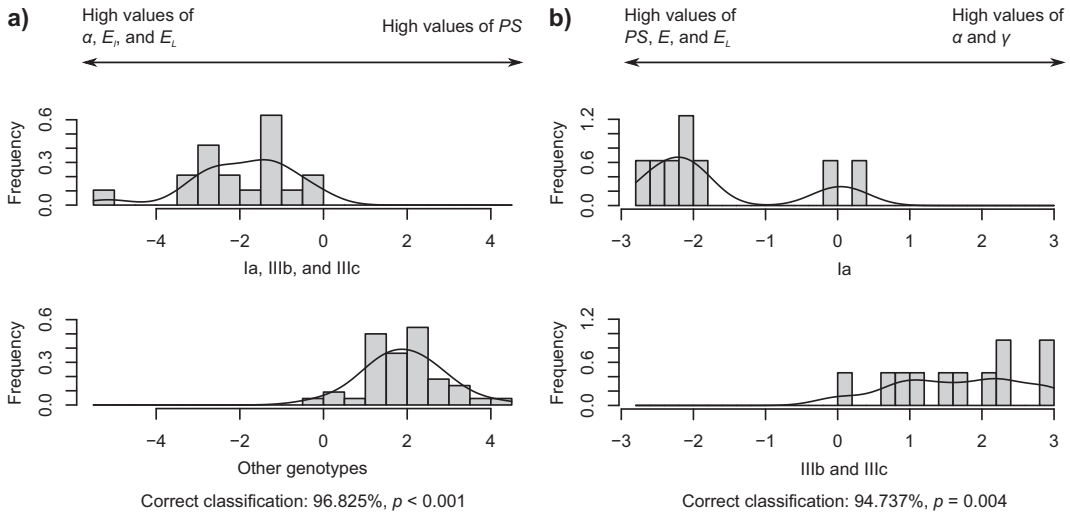

Fig. 7. LDA histograms for morphological distinction between selected genetic types of the *Globigerinella siphonifera*/*G. calida* plexus. a) Histograms of linear discriminant analysis (LDA) between the genetic Types Ia + IIIb + IIIc and the other genetic types. Genetic Types Ia + IIIb + IIIc are characterized by a stronger elongation of the last chamber in both lateral and umbilical/spiral view. b) Histograms of LDA between the genetic Types Ia and IIIb + IIIc, showing that Types IIIb + IIIc are characterized by the larger value of α (inversely correlated with *PS*), i.e. by a more trochospiral coiling and a less equatorial aperture.

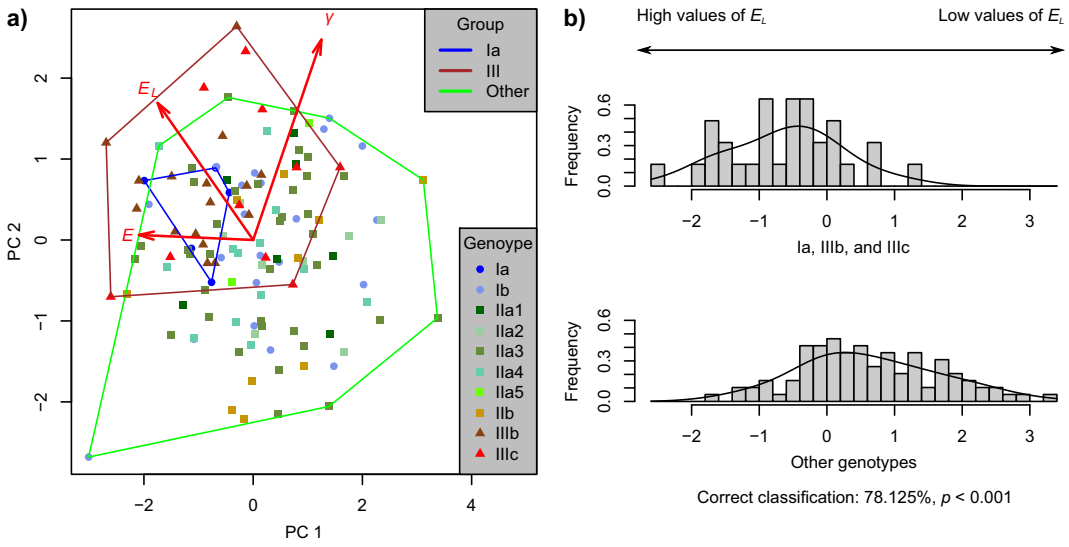

Fig. 8. PCA biplot and LDA histograms of morphometric data obtained from light microscopic images of *Globigerinella siphonifera*/*G. calida* individuals. a) Principal component analysis (PCA) of three size-invariant characters (see Fig. 3) extracted from light microscopic images in umbilical/spiral view. Types Ia and III are situated in one sector of the plot and are mainly distinguished from the other genetic types by a stronger elongation of the last chamber, albeit showing large overlap in morphospace with the other types. b) Linear discriminant analysis (LDA) histograms for the distinction of genetic Types Ia + IIIb + IIIc from the other types on the basis of the three characters extracted from light microscope images. The correct classification rate in the LDA is larger than 78%, and the Hotelling's T2 value indicates a significant morphological difference between the groups. Nevertheless, the large overlap between the histograms confirms the PCA results indicating that distinctions between the genetic types on the basis of umbilical/spiral light microscopic images alone is less reliable than that based on exactly positioned SEM images including the lateral view.

measured per individual. Comparing the mean pore diameter and the mean porosity with the size of the individuals we see a trend towards increasing pore parameters with larger shell sizes, when regarding the whole plexus as a single group ($p < 0.001$, Fig. 9). When the different genetic types are regarded as separate entities, however, this trend is only significant in Types IIa4 ($p_{(\text{pore size})} = p_{(\text{porosity})} = 0.028$), and IIa5 ($p_{(\text{porosity})} = 0.005$, Table S3). In the majority of size classes we detect the whole range of pore size and porosity values. The use of a mathematical approach to calculate the pore parameters of specimens of the *G. siphonifera*/*G. calida* plexus on the basis of measurements that are widely independent of the viewing angle makes our results reliable, even though we could in rare cases only measure 10 pores/specimen. This is supported by the high degree of replicability of measurements on the same specimen ($n = 40$, paired *t*-test, $p_{(\text{pore size})} = 0.789$, $p_{(\text{porosity})} = 0.912$).

Testing for possible influences on the pore parameters using a Scheirer–Ray–Hare test, we detected a significant influence of the genetic background of the individuals as well as of the region in which they were sampled, but not of the interaction term of the two factors (Table 1). We observe large pore diameters and high porosity in individuals belonging to Types Ia and Ib and small pores and low porosity values in the morphologically similar Types IIIb and IIIc (Fig. 10, Table S3). The genetic Type cluster IIa is marked by a high variability in pore sizes and porosities within genetic types, with three Types (IIa1, IIa3, and IIa4) showing lower values than Type IIa5. Comparing the different sampling localities, we detect smaller pore sizes and porosity values in the Pacific and off Japan compared to the Indian Ocean and the Mediterranean Sea. This finding is consistent for all genetic types, which implies that they exhibit the same direction of reaction of the pore parameters to the environmental conditions at a certain sampling locality.

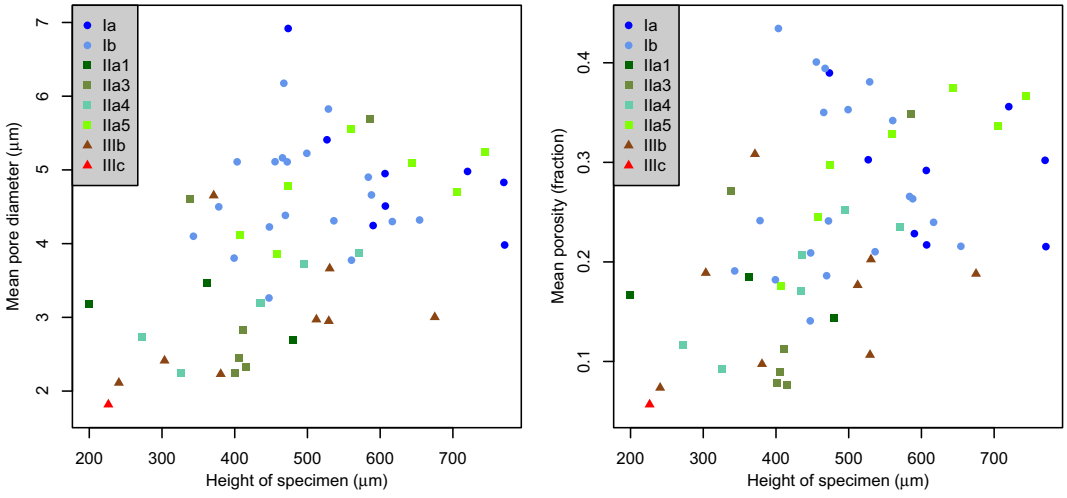

Fig. 9. Relationship between pore parameters and shell size in individuals of the *Globigerinella siphonifera*/*G. calida* plexus. The relationship between pore size and porosity to shell size in the *G. siphonifera*/*G. calida* plexus. Though there is likely a relationship between shell size and pore parameters (due to the small sample sizes this is only significant in Types IIa4 ($p_{(\text{pore size})} = p_{(\text{porosity})} = 0.028$), and IIa5 ($p_{(\text{porosity})} = 0.005$), Kendall–Theil robust line fitting), the graph shows that in the majority of the size range the whole observed range of pore sizes and porosities is realized and the observed variation in these parameters is not merely reflecting shell size.

Table 1
Results of a Scheirer–Ray–Hare test for the influence of genetic type, sampling region, and their interaction on the pore size and porosity of specimens of the *Globigerinella siphonifera*/*G. calida* plexus. For a full cross-wise comparison of genetic types and sampling sites (Mann–Whitney *U* test with adjusted *p*-values) see Table S3.

Factor	*p*-Value (pore size)	*p*-Value (porosity)
Genetic type	<0.001	<0.001
Region	0.008	0.008
Genetic type * Region	0.100	0.053

4. Discussion

4.1. Representativeness of sampling

To date, *Globigerinella* appears to be the most genetically diverse genus within the planktonic foraminifera (Figs. 1, 5; de Vargas et al., 2002; Darling and Wade, 2008). However, the amount of genetic diversity is not endless and a Jackknifing analysis presented by Weiner et al. (2014) indicated that the 12 genetic types recorded at that time were likely a comprehensive representation of the genetic diversity within the lineage. In this study, DNA sequences were obtained from an additional 44 individuals from three stations in the southern Pacific, a region that was not sampled before. Yet, all of these sequences could be assigned to one of the genetic types of Weiner et al. (2014). This fact supports the claim by Weiner et al. (2014) that the number of sampled genetic types is close to saturation both with respect to the addition of more individuals as well as to sampling of new regions. This is important, because it allows us to assume that the image dataset we analyze is representative of the full diversity within the plexus.

4.2. Genetic identity of *G. calida* specimens

Due to the morphological similarity between *G. calida* and *G. siphonifera*, the genetic distinction between the two morphospecies remained uncertain. However, an analysis of the original attributions given to each sampled individual included in this study indicated that the *G. calida* morphology, mainly characterized by more elongated chambers (Parker, 1962), is found in several of the delineated genetic types (Types Ia, IIIb/c, Figs. 4 and 5). This analysis also revealed that the specimens have been labeled as *G. calida* conservatively, i.e., the majority of the specimens belonging to the genetic types associated with the *G. calida* morphology were labeled as *G. siphonifera* (Table S1).

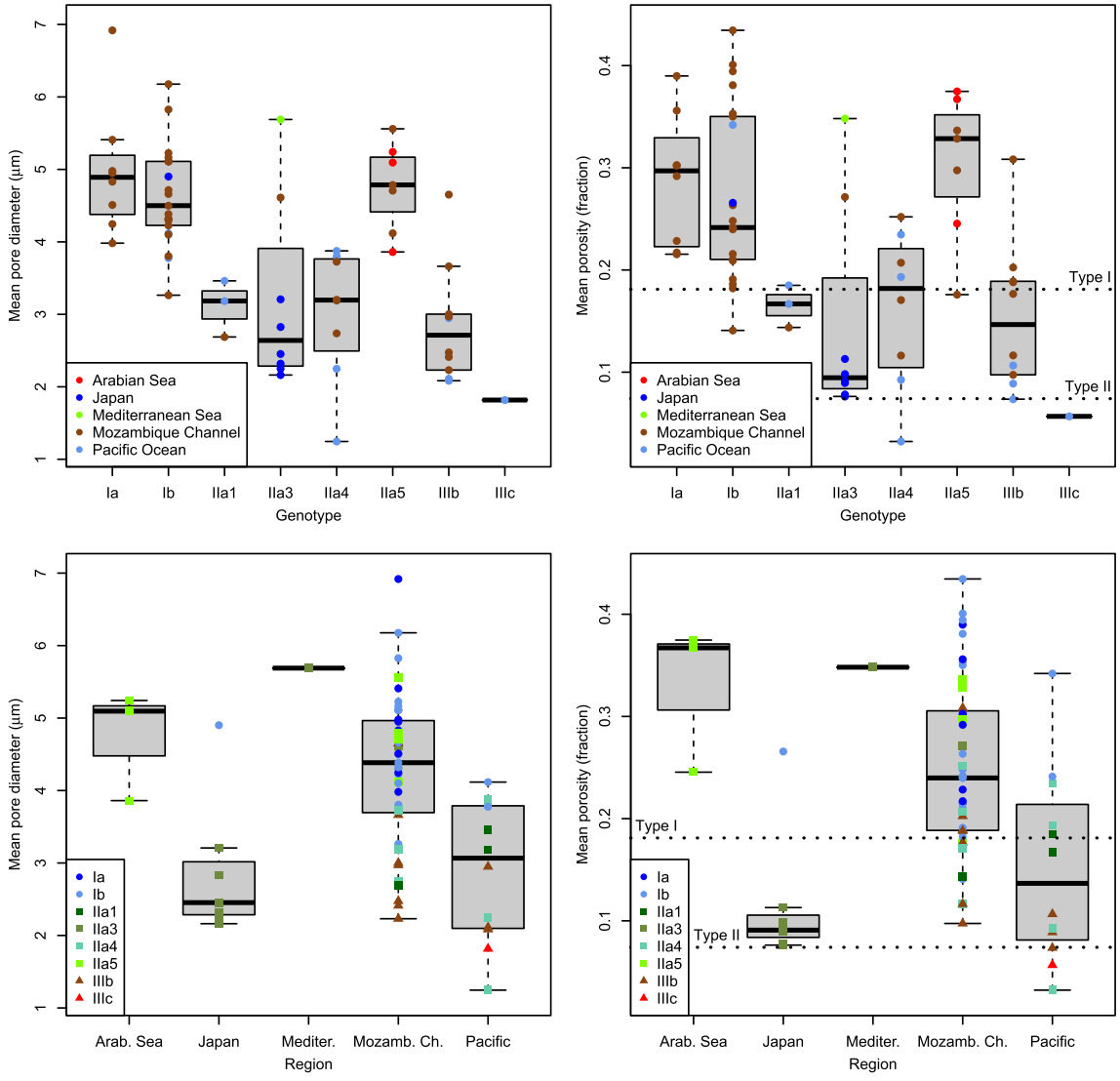

Fig. 10. Boxplots for the analysis of influence of genetic type and sampling location on the pore parameters in *Globigerinella siphonifera*/*G. calida* individuals. Boxplots and original data points showing the variability of pore size and porosity within the *G. siphonifera*/*G. calida* plexus by genetic type and sampling location. Both genetic type and sampling location have a significant influence on both parameters (Table 1). In the porosity plots the porosity values determined by Huber et al. (1997) as being typical for the last chamber of their Types I and II are indicated by dotted lines.

This is interesting considering that the SEM-based morphometric analysis revealed a strong separation of specimens with the general *G. calida* morphology (Fig. 7a). Conversely, the analysis based on light microscope images (Fig. 8) showed a higher degree of overlap between the two groups, indicating that the distinction between the two morphospecies is less obvious when it is difficult to orient the shells freely, such as when taking images of living specimens from the plankton.

The analysis of the genetic identity of specimens labeled as *G. calida* in the field (Figs. 4) and the morphometric analysis (Fig. 7a) both indicate that the general morphology of *G. calida* occurs independently in two unrelated lineages. Moreover, specimens belonging to these lineages can clearly be separated from each other morphologically using SEM images (Fig. 7b). Since this separation is based on a character that is only visible in the lateral view, a validation on light microscopic images was not possible. Nevertheless, specimens in the field can be observed in lateral views and the character is thus likely to be useful in field studies as well.

The association of two distinct "*G. calida*" morphologies with two genetically distinct lineages underlines the existence of a taxonomic confusion. Before any attempt to resolve this confusion, it has to be established that the morphological differences do not represent ecophenotypic variants. This possibility can be easily discarded on the basis of our sampling. Specimens belonging to all three morphologically recognizable groups co-occur at the same stations and depth intervals (Fig. 2, Table S1). If the characters associated with the broad "*G. calida*" morphology were due to ecophenotypic variability then there should have been no distinction between specimens of the *G. siphonifera* and *G. calida* morphology from the same plankton haul.

4.3. Congruence of morphotypes with existing species concepts

To clarify the relation of the three morphotypes to the original morphological concepts we projected the morphometric values of the type specimens and illustrations onto the PCA plot, revealing a surprisingly high congruence with the three morphologic groups (Fig. 6). The *G. siphonifera* morphology appears to be most akin to the largest group of genetic types, especially when the lectotype by Banner and Blow (1960) is considered. The lectotype specimen has been selected by these authors out of the original material of d'Orbigny (1839). It represents a typical specimen of what has been in their opinion commonly associated with the name *G. siphonifera*, and a better congruence of the lectotype than the original drawing by d'Orbigny (1839) with our samples is thus not surprising. Since the exact specimen illustrated by d'Orbigny (1839) as *G. siphonifera* cannot be clearly identified within his collection, the lectotype by Banner and Blow (1960) must be considered as the type of this species. Consequently, we conclude that most of our genetic types correspond to the current morphospecies concept of *G. siphonifera* and the lectotype of the species selected by Banner and Blow (1960) indeed represents a fair representation of the morphology of this taxon.

The separation of the two "*G. calida*" morphologies is possible on the basis of characters best seen in the lateral view. Individuals of the genetic Types IIIb and c are characterized by a higher deviation from planspirality than individuals belonging to Type Ia and are therefore closer to the original description of the *G. calida* morphology, which was described as having an umbilical aperture (Parker, 1962). This is supported by the fact that the *G. calida* holotype is projected very close to the IIIb/c group in the PCA biplot. In order to further test our assumption that the genetic lineage III corresponds to *G. calida*, we used molecular clock estimates to compare the ages of the lineages derived from molecular data to those observed for morphospecies in the fossil record (Fig. 11; Weiner et al., 2014). The first appearance of *G. calida* in the fossil record lies between 3 and 4 Ma according to the CHRONOS database (http://chronos.org), *G. praecalida* first occurred at about 9 Ma. These ages are consistent with the *G. praecalida* morphology representing ancestral populations of lineage III, their first appearance marking the divergence between lineage III and lineage II. In this scenario, interestingly, the appearance of the *G. calida* morphology around 3 Ma corresponds to the oldest divergence among the genetic types of lineage III. Importantly, the fossil record is not compatible with the divergence age of lineages Ia and Ib, which is too young. If lineage Ia represented *G. calida*, then that morphology would have to be associated with lineage I until the divergence between genetic Types Ia and Ib, when Type Ib would have lost its chamber elongation. We consider this scenario less likely, because it would imply that the morphology of genetic Type Ib would have to revert back to the ancestral morphology (the ancestral Miocene form of *Globigerinella*, *G. obesa*, does not possess radially elongated chambers). These observations further support the assumption that extant representatives of the genetic lineage III best represent the morphospecies concept of *G. calida* as it has been applied in the fossil record.

Since the genetic Type Ia can also be separated morphologically from all other types we investigated whether it is related to some already known morphologic concept. *Globigerinella adamsi* was described as a sister to *G. siphonifera* and *G. calida* (Banner and Blow, 1959) and could be a potential candidate. However, *G. adamsi* is described as having even more elongated chambers (Banner and Blow, 1959; Parker, 1962) and so far it was exclusively found in sediments from the Pacific or Indian Ocean (Bé and Tolderlund, 1971; Hemleben et al., 1989). Since we find our Type Ia also in the Caribbean Sea, *G. adamsi* is unlikely to correspond to it.

Searching the literature we discovered with *Globigerina radians* (Egger, 1893) an illustration of a specimen possessing a morphology that closely resembles that of *G. calida* but appears more planispiral. Adding the morphometric parameters of the type illustration to the PCA we found that the illustration corresponds to our specimens of Type Ia, characterized by highly elongated chambers and a small value of α. While the type specimen of *G. radians* arguably plots on the margin of the morphospace occupied by type Ia, this offset may be the result of the poor image quality, which hampered the extraction of the necessary morphological parameters and may have resulted in a slight overestimation of the true chamber elongation in that species. We further note that the original description of *G. radians* by Egger (1893) appears indistinguishable from the description of *G. calida* by Parker (1962), but the distinctly planispiral specimen illustrated by Egger (1893) differs from the holotype of *G. calida* (Fig. 6). We therefore propose to reinstate *G. radians* as a name for specimens of genetic Type Ia (Fig. 12).

To compare our morphotypes with the two types that were first described by Faber et al. (1988) and morphometrically analyzed by Huber et al. (1997), we projected the morphological traits of one specimen of Type I as well as Type II, figured in Huber et al. (1997, Fig. 7), into the PCA morphospace of our analysis (Fig. 6). Thereby we could show that their Type II resembles our *G. siphonifera*, whereas their Type I is closer related to our *G. radians*.

4.4. The paraphyletic status of G. siphonifera

A taxonomic revision of the *G. siphonifera*/*G. calida* plexus is confounded by the fact that the morphology of several genetic types cannot be evaluated (Table 2). Thus, genetic Type IIIa did not yield images of a high enough quality to be included in the morphometric analyses. It can therefore not be ruled out that this genetic type is associated with the *G. siphonifera* morphology rather than *G. calida* like the rest of lineage III. Further difficulty arises from the fact that the majority of the genetic types appear morphologically similar. This is most troublesome for Type Ib, which cannot be included into the morphospecies concept of *G. radians*, because it resembles the *G. siphonifera* morphology otherwise found in specimens of lineage II. Consequently, our taxonomic revision based on shell morphology (Fig. 6) leads to a paraphyly in *G. siphonifera*, where the taxon includes specimens of genetic Type Ib and lineage II, which are unrelated, but cannot be separated morphologically from each other (see Fig. S1). It is entirely possible that traits other

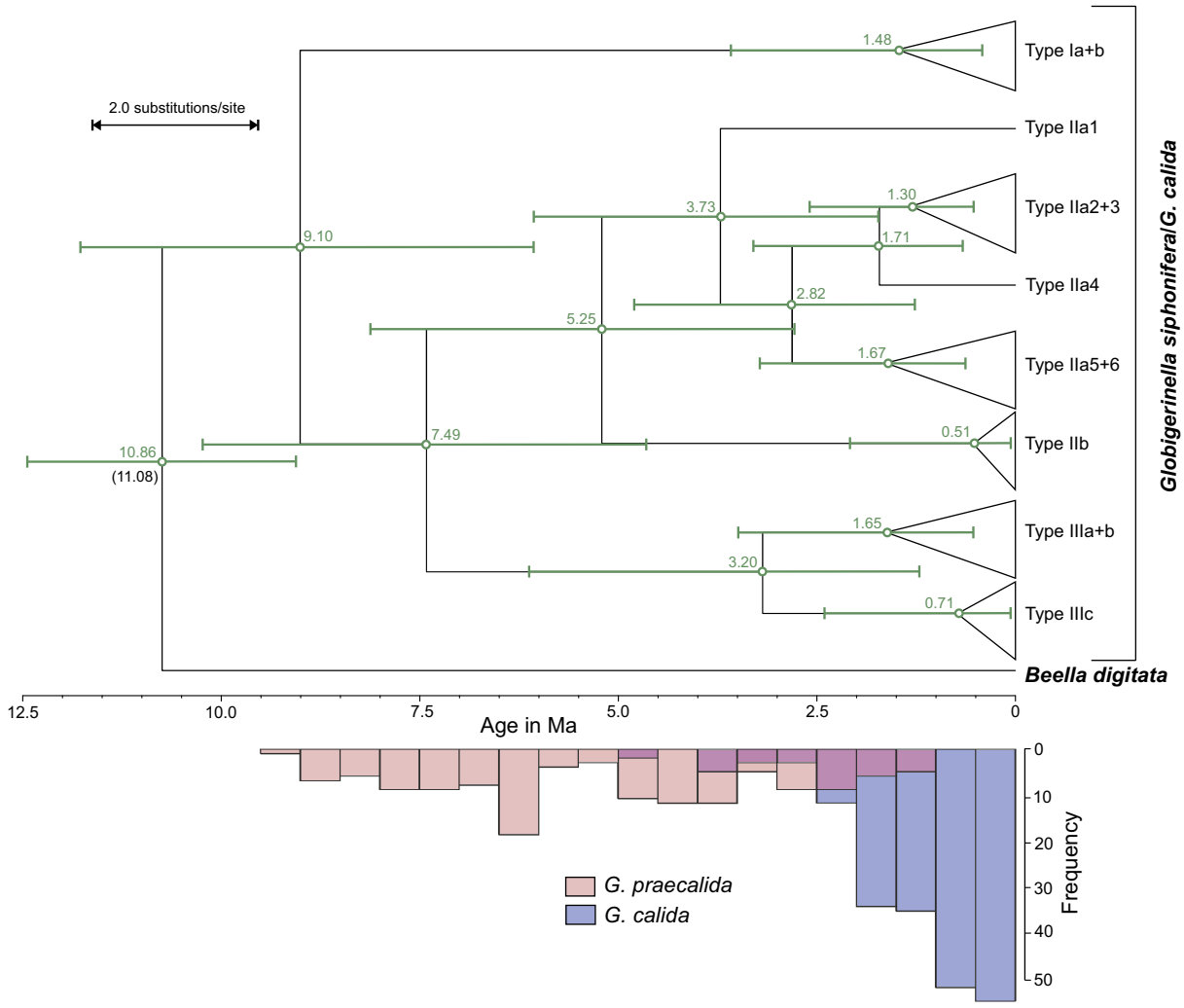

Fig. 11. Molecular clock estimates for *Globigerinella siphonifera*/*G. calida* and their sister species *Beella digitata*. Molecular clock for *G. siphonifera*/*G. calida* and *B. digitata* based on a MAFFT alignment with time estimate ranges from the uncorrelated lognormal relaxed molecular clock, modified after Weiner et al. (2014). For details on the procedures see this previous study. Numbers at nodes indicate divergence ages with 95% confidence intervals. Number in brackets indicates fixed age for the split of *Globigerinella* and *B. digitata*. The histogram shows the occurrence of *G. calida* (blue) and *G. praecalida* (red) as it is recorded in the CHRONOS database (http://chronos.org). (For interpretation of the references to color in this figure legend, the reader is referred to the web version of this article.)

than those based on shell morphology will allow a separation of Type Ib from *G. siphonifera* and we note that biological or physiological differences (including the possession of symbionts), were shown before to diverge between two different types of *G. siphonifera* (Faber et al., 1988, 1989; Huber et al., 1997).

In this context, a feature of the shell that was reported to differ between the two different types originally described by Faber et al. (1988) is the shell porosity (Huber et al., 1997). Differences in pore size were used to differentiate between the two types for which also a relationship to genetic divergence was suggested. In the present study we use porosity measures as a further set of characters to differentiate genetic types on a morphological basis and to assess the correlation with the Types I and II as described by Faber et al. (1988). Because pores appear to facilitate gas exchange between the cytoplasm and the environment (Hemleben et al., 1989), shell porosity is primarily controlled by body size (Brummer et al., 1987). This is because cytoplasm volume increases with the cube of chamber diameter, but pore area only with the square of chamber diameter. This relationship explains the observed relationship between porosity and shell size in our data (Fig. 9). However, within the range of shell sizes represented in our dataset, we only detected a minor influence of shell size on pore parameters, explaining a maximum of 23% of the total variation (Fig. 9, Table S3). Therefore, we conclude that among the studied specimens porosity is not predominantly controlled by the individual ontogeny, and the observed differences require another explanation. Taking other parameters into account, both the genetic type and the sampling location have a significant influence on the pore parameters (Table 1). Especially, there is a strong genetic influence with five of the eight analyzed genetic types consistently showing low porosity values (Fig. 10).

The largest pores and higher porosity is observed in specimens of lineage I. This is consistent with the results by Huber et al. (1997), suggesting that pore parameters could be used to differentiate specimens of genetic lineage I from specimens of lineage II. The values of mean porosity reported for the two genetic types in Huber et al. (1997) are slightly lower than those observed among the analyzed specimens (Fig. 10). This offset likely reflects the fact that we measured the pores from the outside instead of breaking the shell to measure from the inside. We observe that large pores and high porosity also marks specimens of genetic Type IIa5 (Fig. 10). This means that the propensity for building disproportionately large and more concentrated pores evolved at least twice in *Globigerinella* and cannot be universally used to differentiate between specimens of lineages I and II. On the other hand, the

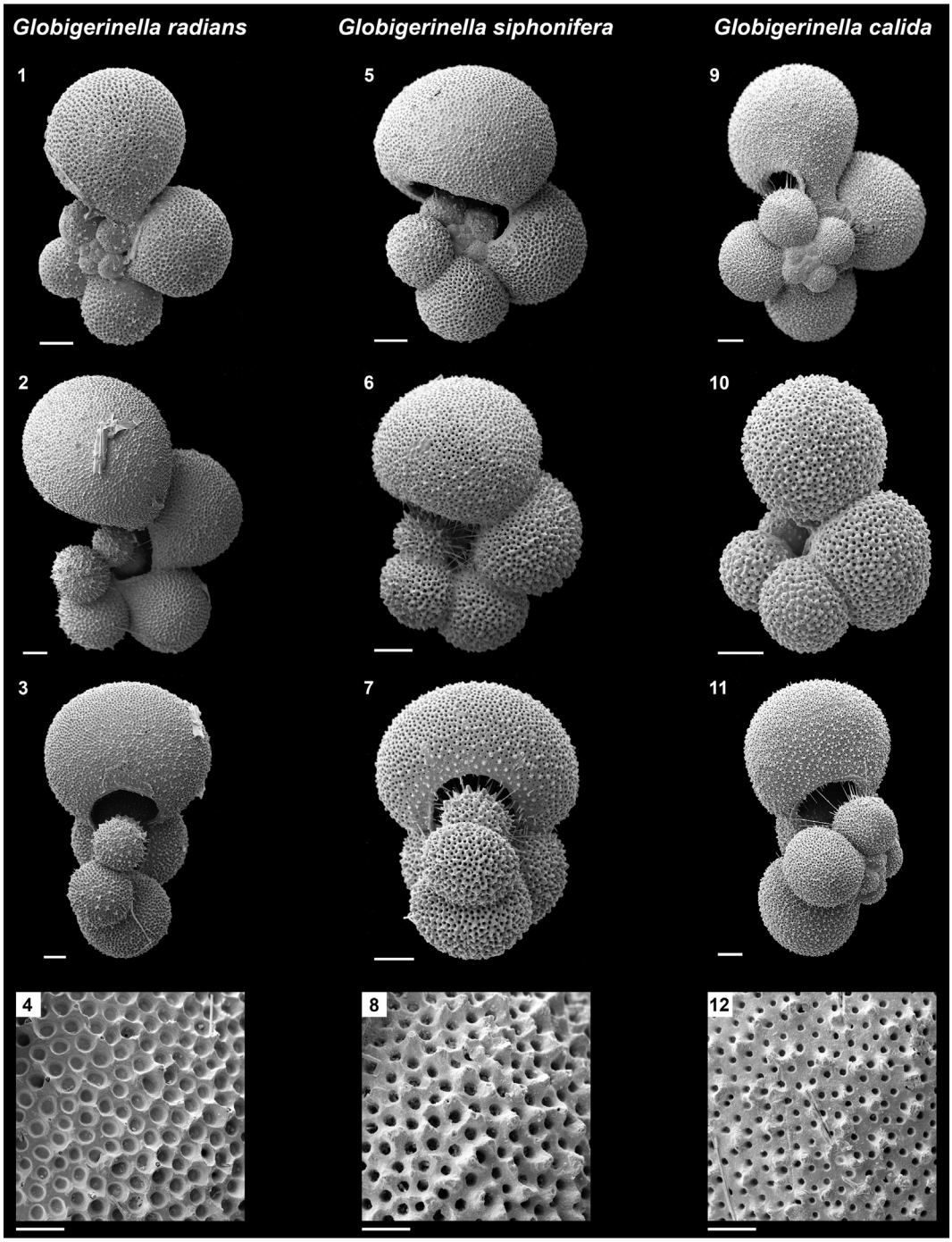

Fig. 12. SEM images of the three morphotypes. SEM images of the spiral, umbilical and lateral view and close-up view of the pores of two individuals of each morphotype with their revised taxonomy. Scale bars at pictures with the whole shell are 60 μm, close-ups have a scale bar of 20 μm. *Globigerinella radians* specimens originate from the Mozambique Channel, stations MC-4 (1) and GLOW 5 (2–4), *Globigerinella siphonifera* specimens from the Mozambique Channel, station MC-11 (5) and the Arabian Sea, station 945 (6–8) and *Globigerinella calida* specimens from the Mozambique Channel, stations MC-12 (9, 11, 12) and MC-4 (10).

observation that there is no statistically significant interaction between genetic type and sampling region suggests that the observed differences in pore parameters are an inherent property of the genetic types and are at least partly genetically fixed. The existence of a weaker but significant relationship between pore parameters and locality implies a secondary ecophenotypic effect. This effect is consistent between genetic types (has the same sign), meaning that the pore parameters will remain offset at the same locality and may be used as a rough indicator to distinguish between the genetic Types I + IIa5 and rest of II + III, even though the threshold value will differ among localities.

4.5. Ecological differentiation

In many cases, genetic types were shown to exhibit a more restricted biogeographical distribution than the morphospecies they belong to (e.g. Aurahs et al., 2009; Weiner et al., 2012). De Vargas et al. (2002) reported a non-random distribution associated with the productivity in the water column for four different genetic lineages of *G. siphonifera*, corresponding to our lineages I, IIa, IIb and III. Therefore, we also tested for a potential correlation between the distribution of the revised morphospecies and water mass characteristics. However, the fact that in

Table 2
The correspondence between genetic diversity and morphological variability within the *Globigerinella siphonifera*/*G. calida* plexus, including classification following classical taxonomy (e.g., Parker, 1962) and the revised taxonomy, based on the morphometric measurements from this study. Question marks stand for genetic types whose morphology could not be confirmed by quantitative analysis, because no suitable images were available.

Genetic type	Revised taxonomy	Classical taxonomy
Ia	*G. radians*	*G. calida* or *G. siphonifera*
Ib	*G. siphonifera*	*G. siphonifera*
IIa1	*G. siphonifera*	*G. siphonifera*
IIa2	*G. siphonifera*	*G. siphonifera*
IIa3	*G. siphonifera*	*G. siphonifera*
IIa4	*G. siphonifera*	*G. siphonifera*
IIa5	*G. siphonifera*	*G. siphonifera*
IIa6	?	*G. siphonifera*
IIb	*G. siphonifera*	*G. siphonifera*
IIIa	?	*G. calida*
IIIb	*G. calida*	*G. calida*
IIIc	*G. calida*	*G. calida*

many regions all three morphospecies co-occur indicates that there is no difference in their biogeographic distribution and their co-occurrence in the same depth intervals excludes a potential vertical separation pattern in the water column. A comparison with data from surface sediment samples as reported in the MARGO database (Fig. 2, Barrows and Juggins, 2005; Kucera et al., 2005) also shows that *G. siphonifera* and *G. calida* share a common range of occurrence.

To test specifically for a possible affinity to different environmental settings between the two species with elongated chambers, we plotted the localities of all genotyped specimens (Weiner et al., 2014 and this study) of these morphospecies against the annual average temperature and productivity at those localities. By comparing the occurrence of *G. calida* and *G. radians* in the north Atlantic, Mediterranean Sea and Caribbean Sea with extracted sea surface temperature and chlorophyll a data we observe the exact same temperature tolerance of both *G. calida* and *G. radians* (Fig. 13). Both morphotypes show two abundance peaks, one at a higher temperature and one in colder waters. When comparing those results with the distribution of "*G. calida*" in the sediment according to the MARGO database it appears that this pattern resonates with the occurrence of two abundance maxima in the morphospecies. Therefore, the "*G. calida*" assemblages seem to be a mixture of *G. calida* and *G. radians*.

4.6. Parallel evolution of morphological traits

By comparing the morphology of the individuals to their genetic background we were able to support our first impression that morphological divergence only maps partly onto the genetic diversity. We find elongated chambers in individuals of lineages I and III, leaving only lineage II to completely represent the typical *G. siphonifera* morphology. Thus, unexpectedly, we are confronted with the fact that a similar chamber morphology evolved twice in *Globigerinella* and can be found in individuals belonging to different genetic lineages. The same seems to apply to the evolution of larger pores and higher porosity. This character has likely evolved early (late Miocene) in the evolutionary history of lineage I, but it also must have evolved in parallel in genetic Type IIa5, most likely in the Quaternary (Fig. 11). We suggest that the evolution of elongated chambers in two different genetic lineages is the result of parallel evolution, as it was shown before to have been the case for digitate chamber shapes in various morphospecies of planktonic foraminifera (Coxall et al., 2007) as well as for certain keel structures that appeared independently in closely related lineages (Norris, 1991a). The pervasive appearance of parallel evolution in foraminifera shell morphology might either be the result of developmental constraints that allow for only a certain number of possible shapes or of directional evolutionary trends shaped by environmental forces (compare Norris, 1991b). Elongated chambers were argued to likely represent an adaptation to feeding in the low productivity subsurface regions of the water column (Coxall et al., 2007). However, *G. calida* as well as *G. radians* both occur in surface waters, suggesting that the formation of elongated chambers not necessarily indicates a deep dwelling habitat. Surprisingly, in the genus *Globigerinella* we show that parallel evolution operates on the lowest taxonomic level, and that it involves not only chamber shape but also the properties of the shell wall (pore parameters).

5. Conclusions

The morphometric analysis of shell shape and porosity of genotyped individuals of the *Globigerinella siphonifera*/*Globigerinella calida* plexus provides evidence for the morphological differentiation of several SSU

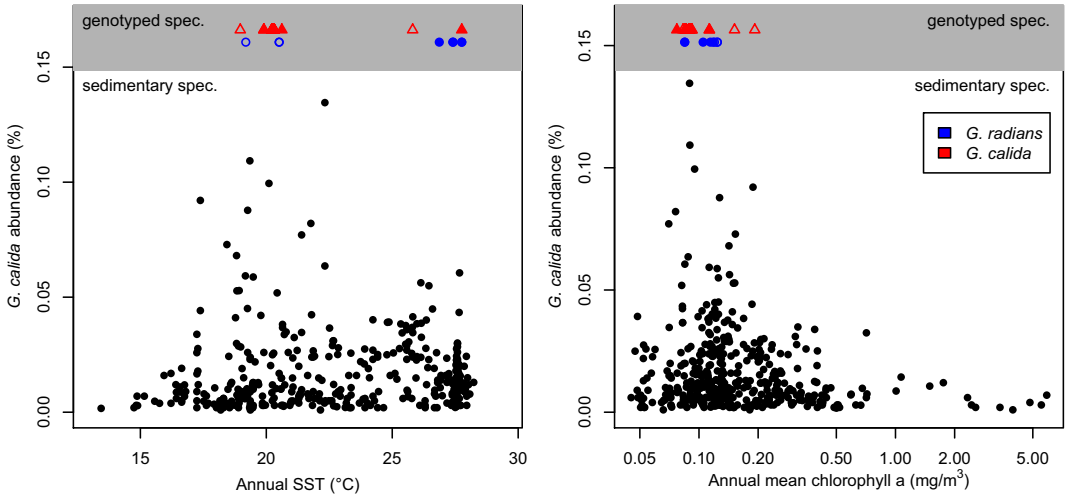

Fig. 13. Distribution of *Globigerinella calida* and *G. radians* along sea surface temperature and primary productivity. Distribution of the morphotype generally referred to as *G. calida* (Barrows and Juggins, 2005; Kucera et al., 2005) along sea surface temperature (global SST as annual mean and mean of the upper 20 m of the water column from the World Ocean Atlas, Locarnini et al., 2013) and productivity (10-year averaged annual chlorophyll a concentration from Ocean Color Web, Feldman and McClain, 2013) in the Northern Atlantic (including Caribbean) and the Mediterranean Sea. Corresponding SST and chlorophyll a values for the sampling sites of genotyped and morphologically analyzed individuals of *G. calida* and *G. radians* from this study are added at the top of the graphs (filled symbols: genetic type and morphotype known, open symbols: only genetic type known). Both morphospecies appear to show the same preferences for primary productivity as well as water temperature.

rDNA genetic types. A detailed morpho-genetic comparison allows us to use this information to revise the taxonomy of the genus. Our analyses show that the genetic Types Ia, IIIb and IIIc can be separated from the rest of the altogether 12 genetic types due to their radially elongated chambers and in case of Types IIIb/c also because of the high deviation from planspirality. Although a separation into three morphologic groups proved to be difficult using light microscopic pictures, the differentiation conducted on SEM images is highly significant. We also discovered a difference in the porosity and pore size values between the different genetic lineages. However, our data show that the pore parameters are influenced not only by the genetic background of the individual but also by environmental factors and that like chamber shape this character also underwent parallel evolution. A comparison of the three morphologic groups with the original descriptions for members of the *Globigerinella* genus reveals that most of our genetic types correspond to the morphology of *G. siphonifera*. The genetic lineage III could be shown to most resemble the true *G. calida* morphology (Parker, 1962), which is also supported by molecular clock estimates, dating the diversification in this lineage to the same age as the appearance of *G. calida* in the fossil record. For the third morphologic group found within the plexus, we propose the name *Globigerinella radians*, which was attributed to this morphology by Egger (1893) but virtually ignored since. We are aware of the fact that a revision of the taxonomy in *Globigerinella* creates a paraphyletic group with genetic types of two different lineages manifesting the *G. siphonifera* morphology, but our data do not show sufficient evidence for a separation of genetic Type Ib from the rest of the *G. siphonifera* group. The fact that we observe elongated chambers as well as high porosity in different genetic types shows that in the genus *Globigerinella* parallel evolution is highly prevalent acting on the lowest taxonomic level.

Supplementary data to this article can be found online at http://dx.doi.org/10.1016/j.marmicro.2014.10.003.

Acknowledgments

We thank the captain, crew and the scientists of cruises on RV *Poseidon* (P349 and 411), *Meteor* (M69/1, 71/2, 71/3, 74/1a,b and 78/1), *Maria S. Merian* (MSM 15/5), *Sonne* (SO226/3), *Pelagia* (64PE303 and 65PE304) and *Tansei-Maru* (KT07-14) for their help in taking plankton samples. We also thank the colleagues from the IUI Marine Station in Eilat, Israel for their help in sampling. Technical assistance of Margret Bayer and Petra Witte in taking SEM images and Michael Siccha in extracting oceanic chlorophyll data is gratefully acknowledged. We thank Alexander Altenbach and Winfried Werner from the LMU Munich and the "bayerische Staatssammlung für Paläontologie und Geologie" for their help in searching for type material. Thanks to Helen Coxall and one anonymous reviewer for very helpful comments on the manuscript. The work was financially supported by the Deutsche Forschungsgemeinschaft (grant KU 2259/19) and the Natural Environment Research Council of the UK (grants NER/J/S/2000/00860 and NE/D009707/1).

Appendix 1. Systematic appendix

1.1. Genus Globigerinella Cushman, 1927

The genus *Globigerinella* as described by Cushman (1927) includes morphospecies of planktonic foraminifera with nearly planispiral tests in the adult stage, globular to ovate chambers, umbilical to equatorial aperture and fine rounded spines (Kennett and Srinivasan, 1983). Three extant morphospecies have been assigned to this genus (e.g. Hemleben et al., 1989): *Globigerinella siphonifera* (d'Orbigny, 1839), *Globigerinella calida* (Parker, 1962) and *Globigerinella adamsi* (Banner and Blow, 1959). In the present study based on genetic and morphometric data, we further include among the extant species of the genus *Globigerinella radians* (Egger, 1893).

1.2. Globigerinella radians (Egger, 1893)

Figs. 12, 1–4.

Globigerina radians Egger, 1893, p. 170, plate XIII (Figs. 22–24).

Non *Globigerina radians* — Rhumbler, 1909, p. 148, plate XXIX (Figs. 2–4) — Parker, 1958, p. 278, plate 5 (Fig. 10) — Drooger and Kaasschieter, 1958, p. 84, plate 4 (Fig. 24) plate 5 (Fig. 6).

1.2.1. Type specimen

None designated; the specimen figured by Egger (1893) on plate XIII, Figs. 22–24 is based on material of the Gazelle expedition from 1874 to 1876, which was stored at the "bayerische Staatssammlung für Paläontologie und Geologie", but destroyed during second world war; the original type material is thus considered to be lost.

1.2.2. Type locality

The morphospecies was originally described from sediments from the southern Indian and Pacific Ocean collected during the Gazelle expedition from 1874 to 1876, localities cited in Egger (1893) are west. Australia St. 87 (20°49 S, 113°46 E, depth 915 m), St. 90 (18°52 S, 116°18 E, depth 357 m); Fiji St. 130 (14°52 S, 175° 32 W, depth 1655 m).

1.2.3. Original description

"Die Schale erreicht 0.35 Millimeter Höhe bei 0.27 Breite, findet sich selten in grösseren, häufig in kleineren Dimensionen. Sie kennzeichnet sich durch einen eigenthümlich losen Aufbau, welcher in der letzten Windung vier bis fünf kaum zusammenhängende, in der Regel mit ihrer längeren Achse senkrecht zum Mittel der Schale gerichtete Kammern hat. Das Wachstum dieser Kammern nimmt sehr rasch zu, die letzte Kammer ist viel grösser als die vorhergehende, und so zurück. Die Anfangswindung ist nur dürftig entwickelt. Die Seiten sind flach, die Nabelfläche ist wohl vertieft, aber in der Mitte völlig offen. Die Oberfläche ist rauh, stachelig. Von *Globig. digitata* unterscheidet die Form der hier gerundeten, dort zugespitzt verlängerten Kammern, von *Globig. aequilateralis* die seitliche Aufrollung, die strahlig abstrebende Kammerstellung. *Glob. quadrilobata* d'Orb. hat gleichmässigere Kammergrösse und stets nur vier Kammern." (Egger, 1893, p. 170).

1.2.4. Translated original description

The shell is up to 0.35 mm high and 0.27 mm wide, but few shells reach that size while many remain smaller. The very lobate shell is composed of 4–5 loosely arranged chambers in the last whorl, with a distinct radial chamber elongation and a high relative size increase from chamber to chamber. The initial spiral is diffuse, the spinose shell is laterally flattened and evolute. The species is distinguished from *G. digitata* by rounded instead of pointed tips of the elongated chambers, from *G. aequilateralis* by the higher trochospirality and the radially elongated chambers, and *G. quadrilobata* has a more constant chamber size and only four chambers.(Egger, 1983, p. 170).

1.2.5. Emended description

The species concept for *Globigerinella radians* is based on the description by Egger (1893), but it is extended in the present study as follows: Individuals of *G. radians* possess nearly planispirally coiled highly evolute shells with typically five chambers in the last whorl. Chambers in the last whorl are radially elongated (mean values: $E_I \approx 0.9$, $E_L \approx 1.1$, $E \approx 1.0$) with rounded tips. Aperture is equatorial, forming a high symmetrical arch. The surface of the shell is covered by round spines. The morphospecies differs from *Globigerinella calida* by a more planispiral coiling (mean values: $\alpha \approx 7.9°$, $PS \approx 0.9$) as well as by possessing larger pores and higher shell porosity. Unlike *Globigerinella adamsi*, *G. radians* never shows pointed chamber tips and the degree of chamber elongation is not as extreme as in that morphospecies.

1.2.6. Mean shell height in lateral view

473–771 μm (mean = 633 μm, $n = 8$).

1.2.7. Observed occurrences in this study (genotyped individuals)

Caribbean Sea, Mozambique Channel, southwestern Pacific Ocean.

1.2.8. Remarks

The original description of *G. radians* by Egger (1893) refers to planispirally coiled shells with a loose chamber arrangement and a significant size increase from one chamber to the next as well as a spinose surface. Subsequently, Rhumbler (1909) used the name *Globigerina radians* for a non-spinose foraminifera, although he is referring to Egger's work (1893). Rhumbler's concept was adopted by (Parker, 1958) until it was renamed as *Globigerina atlantisae* by Cifelli and Smith (1970), and later synonymized with *Tenuitella iota* (Hemleben et al., 1989). Drooger and Kaasschieter (1958) used the name *G. radians* for specimens from Caribbean surface sediments corresponding to a morphology that we consider to be *G. calida*.

1.3. Globigerinella calida (Parker, 1962)

Fig. 12, 5–8.

Globigerina subcretacea — Drooger and Kaasschieter, 1958, p. 84, plate 4 (Fig. 23) plate 5 (Fig. 5).

Globigerina radians — Drooger and Kaasschieter, 1958, p. 84, plate 4 (Fig. 24) plate 5 (Fig. 6).

Globigerina sp. — Bradshaw, 1959, p. 38, plate 6 (Figs. 19, 26–28).

Globigerina calida Parker, 1962, p. 221, plate 1 (Figs. 9–13, 15).

Globigerinella calida — Saito et al., 1976, p. 282, plate 1 (Fig. 2) plate 6 (Fig. 2) plate 8 (Fig. 1) — Saito et al., 1981, p. 32, plate 4 (Fig. 2a–d) — Kennett and Srinivasan, 1983, p. 240, plate 60 (Figs. 7–9) — Hemleben et al., 1989, p. 18, Fig. 2.3 e, f.

1.3.1. Type specimen

Holotype USNM no. 638685 (Parker, 1962).

1.3.2. Type locality

The morphospecies is originally described from surface sediments from the central southern Pacific Ocean (14°44 S, 112°06 W, depth 3120 m), Downwind BG 130 (0–4 cm.)

1.3.3. Original description

"Test trochoid, with a low spire and rounded, highly lobulated periphery: chambers fairly rapidly enlarging, early ones spherical, later ones somewhat elongated radially, 5 in the initial whorl, 4–5 in the final one, up to 15 in the adult test; sutures distinct, depressed, radial on both sides; wall calcareous, radial, perforate, hispid, with long fine spines in living forms; aperture umbilical, semicircular, becoming umbilical–extraumbilical and highly arched in the peripheral plane in some adults, with a narrow lip." (Parker, 1962, pp. 221–222).

1.3.4. Emended description

Parker (1962) describes a typical representative of the species *G. calida*, to which the use in this study is in total agreement. Individuals of *G. calida* possess slightly trochospirally coiled evolute shells with typically five chambers in the last whorl. The last whorl is marked by radially elongated chambers (mean values: $E_I \approx 0.9$, $E_L \approx 1.0$, $E \approx 1.0$) with rounded tips. The aperture is in an interiomarginal position and cannot be seen from the spiral view. The surface of the shell is marked by round spines. The general appearance is similar to *Globigerinella radians*, however, the chambers are less elongated in umbilical/spiral view, the morphospecies has smaller pores and less shell porosity and shows a clear deviation from planispirality (mean values: $\alpha \approx 22.1°$, $PS \approx 0.5$).

1.3.5. Mean shell height in lateral view

226–675 μm (mean = 417 μm, $n = 11$).

1.3.6. Observed occurrences in this study (genotyped individuals)

Caribbean Sea, Eastern Mediterranean Sea, Red Sea, Arabian Sea, Mozambique Channel, middle-western Pacific Ocean.

1.3.7. Remarks

The original description of *G. calida* by Parker (1962) refers to trochospiral shells with rapidly enlarging chambers and the last chambers being elongated radially. Her specimens have ~5 chambers in the final whorl and the apertures are approaching an interiomarginal position. She differentiates *G. calida* from *G. siphonifera* by having less involute chambers and less spines. Parker (1962) synonymizes her description with *Globigerina* sp. described by Bradshaw (1959), however she neither refers to the *Globigerina radians* described in Drooger and Kaasschieter (1958) nor to the *Globigerina subcretacea* from the same authors, which both describe the same morphology as *G. calida*. Parker's description of the morphospecies still remains valid until today, however in Saito et al. (1976) the morphospecies was assigned to the genus *Globigerinella*.

1.4. Globigerinella siphonifera (d'Orbigny, 1839)

Fig. 12, 9–12.

Globigerina siphonifera d'Orbigny, 1839, p. 83, plate 4 (Figs. 15–18).

Cassidulina globulosa — Egger, 1857, p. 296, plate 11 (Fig. 4).

Globigerina aequilateralis — Brady, 1879, p. 285 — Brady, 1884, p. 605, plate 80 (Figs. 18–21) — Egger, 1893, p. 172, plate XIII (Figs. 5–8).

Globigerinella aequilateralis — Cushman, 1927, p. 87 — Bradshaw, 1959, p. 38, plate 7 (Figs. 1, 2) — Cifelli and Smith, 1970, p. 35, plate 4 (Figs. 2–4) — Walker and Vilks, 1973, p. 196, plate 1 (Figs. 6, 7) — Saito et al., 1976, p. 281, plate 3 (Figs. 1, 2) plate 6 (Fig. 7) plate 8 (Figs. 3, 8) — Saito et al., 1981, p. 26, plate 2 (Fig. 2a–d) — Kennett and Srinivasan, 1983, p. 238, plate 59 (Fig. 1) plate 60 (Figs. 4–6).

Hastigerina aequilateralis — Bolli et al., 1957, p. 29, plate 3 (Fig. 4).

Hastigerina siphonifera — Banner and Blow, 1960, p. 22, Figs. 2, 3.

Globigerinella siphonifera — Parker, 1962, p. 228, plate 2 (Figs. 22–28) — Hemleben et al., 1989, p. 18, Fig. 2.3 i, k.

1.4.1. Type specimen

Lectotype: Alcide d'Orbigny collection at the Muséum Nationale de l'Histoire Naturelle, Paris, designated by Banner and Blow (1960).

1.4.2. Type locality

The morphospecies is originally described from recent beach sand on Cuba (Banner and Blow, 1960).

1.4.3. Original description

"*Globigerina*. Testa creberrima, tubulifera, alba; spira plana, loculis tribus sphaericis; apertura elongata. Dimensions: Diamètre 1/3 de millim. Coquille globuleuse, couverte partout d'un grand nombre de petits tubes percés à leur extrémité, qui la rendent comme hérissée. Spire non saillante, composée d'un tour seulement ou de cinq loges à l'âge adulte. Loges sphériques, ou un peu ovales, très distinctes, au nombre de trois au dernier tour. Ouverture en croissant sur le retour et la dernière loge. Couleur, blanc uniforme. Comme les *Globigerina bulloides*, vivant dans l'Adriatique et aux Canaries, cette espèce a quatre loges seulement au dernier tour de spire, caractère que nous trouvons sans exception chez tous les individus; mais elle s'en distingue facilement par les pointes tubuleuses don't elle est couverte: ces mêmes pointes se retrouvent, il est vrai, chez la Globigérine hérissée; mais celle-ci a une toute autre forme, et le dernier tour y est composé de cinq loges." (d'Orbigny, 1839, p. 83).

1.4.4. Translated original description

Shells are thick, tubuliferous, white, planispiral, which places them in the spherical tribus; elongated aperture. Dimension: 1/3 of mm in diameter. Globular shell, covered by a high number of tubes pierced at

their extremity, making it look spiky. The spire is not prominent, composed of one whorl only or five chambers to the adult age. Chambers are spherical, slightly oval, very distinct, at the number of three in the last round. The aperture is at the overgrowth of the last chamber and the preceding whorl. Color, white uniform. As *Globigerina bulloides*, occurring in the Adriatic Sea and the Canaries, this species has always four chambers in the last whorl, feature that we found in all individuals; she is distinguished easily by the tubular spines with which it is covered: the same spines are found on all the spiky Globigerins. But this one has another shape, and the last round is composed of 5 chambers (d'Orbigny, 1839, p. 83).

1.4.5. Emended description

In this study the species concept is used according to Banner and Blow (1960), who describe with their lectotype a typical representative of the species *Globigerinella siphonifera*. Individuals of *G. siphonifera* possess in adult stages nearly planispirally coiled involute shells with typically five chambers in the last whorl. Chambers in the last whorl are globular or ovoid (mean values: $E_I \approx 0.7$, $E_L \approx 0.9$, $E \approx 0.9$). Aperture is equatorial, forming a high symmetrical arch. The surface of the shell is covered with round spines. The morphospecies differs from *G. radians* and *G. calida* by less elongated chambers especially in lateral view. In contrast to *G. calida*, *G. siphonifera* does not show a strong deviation of the growth axis from the planispiral plane (mean values: $\alpha \approx 8.0°$, $PS \approx 1.0$).

1.4.6. Mean shell height in lateral view

200–744 μm (mean = 476 μm, $n = 44$).

1.4.7. Observed occurrences in this study (genotyped individuals)

Caribbean Sea, middle-eastern Atlantic Ocean, Mediterranean Sea, Red Sea, Arabian Sea, Mozambique Channel, western Pacific Ocean.

1.4.8. Remarks

The original description of *Globigerinella siphonifera* by d'Orbigny (1839) refers to planispirally coiled shells with globular chambers and many spines. His specimens have ~5 chambers in the last whorl and the aperture is elongate. The morphospecies was later renamed in *Globigerina aequilateralis* by Brady (1879), however, this name was declared a junior synonym by Banner and Blow (1960). These authors though attributed the morphospecies to the genus *Hastigerina*, which was changed again by Parker (1962), who referred to the morphospecies as *Globigerinella siphonifera*, the name which is still valid today.

References

Agresti, A., Coull, B.A., 1998. Approximate is better than "exact" for interval estimation of binomial proportions. Am. Stat. 52, 119–126.

André, A., Weiner, A., Quillévéré, F., Aurahs, R., Morard, R., Douady, C.J., de Garidel-Thoron, T., Escarguel, G., de Vargas, C., Kucera, M., 2013. The cryptic and the apparent reversed: Lack of genetic differentiation within the morphologically diverse plexus of the planktonic foraminifer *Globigerinoides sacculifer*. Paleobiology 39, 21–39.

Aurahs, R., Grimm, G.W., Hemleben, V., Hemleben, C., Kucera, M., 2009. Geographical distribution of cryptic genetic types in the planktonic foraminifer *Globigerinoides ruber*. Mol. Ecol. 18, 1692–1706.

Aurahs, R., Treis, Y., Darling, K., Kucera, M., 2011. A revised taxonomic and phylogenetic concept for the planktonic foraminifer species *Globigerinoides ruber* based on molecular and morphometric evidence. Mar. Micropaleontol. 79, 1–14.

Banner, F.T., Blow, W.H., 1959. The classification and statigraphical distribution of the Globigerinaceae. Palaeontology 2, 1–27.

Banner, F.T., Blow, W.H., 1960. The taxonomy, morphology and affinities of the genera included in the subfamily Hastigerininae. Micropaleontology 6, 19–31.

Barrows, T.T., Juggins, S., 2005. Sea-surface temperatures around the Australian margin and Indian Ocean during the Last Glacial Maximum. Quat. Sci. Rev. 24, 1017–1047.

Bé, A.W.H., 1977. An ecological, zoogeographic and taxonomic review of recent planctonic Foraminifera. In: Ramsay, A.T.S. (Ed.), Oceanic Micropalaeontology. Academic Press, London, New York, San Francisco, pp. 1–100.

Bé, A.W.H., Tolderlund, D.S., 1971. Distribution and ecology of living planktonic foraminifera in surface waters of the Atlantic and Indian Oceans. In: Funnell, B., Riedel, W. (Eds.), The Micropalaeontology of Oceans. Cambridge University Press, Cambridge, pp. 105–149.

Benjamini, Y., Hochberg, Y., 1995. Controlling the false discovery rate: a practical and powerful approach to multiple testing. J. R. Stat. Soc. Ser. B Methodol. 57, 289–300.

Bijma, J., Hemleben, C., Huber, B.T., Erlenkeuser, H., Kroon, D., 1998. Experimental determination of the ontogenetic stable isotope variability in two morphotypes of *Globigerinella siphonifera* (d'Orbigny). Mar. Micropaleontol. 35, 141–160.

Bolli, H.M., Loeblich, A.R.J., Tappan, H., 1957. Planktonic foraminiferal families Hantkeninidae, Orbulinidae, Globorotaliidae and Globotruncanidae. Bull. US Natl Mus. 215, 3–50.

Bradshaw, J.S., 1959. Ecology of living planktonic foraminifera in the north and equatorial Pacific Ocean. Contrib. Cushman Lab. Foram. Res. 10, 25–46.

Brady, H.B., 1879. Notes on some of the reticularian Rhizopoda of the "Challenger" expedition. 2. Additions to the knowledge of porcellaneous and hyaline types. Q. J. Microsc. Sci. New Ser. 261–299.

Brady, H.B., 1884. Report on the foraminifera dredged by H.M.S. Challenger during the years 1873-1876. H.M.S. Challenger Reports 9, 1–814.

Brummer, G.-J.A., Hemleben, C., Spindler, M., 1987. Ontogeny of extant spinose planktonic foraminifera (Globigerinidae): a concept exemplified by *Globigerinoides sacculifer* (Brady) and *G. ruber* (d'Orbigny). Mar. Micropaleontol. 12, 357–381.

Cifelli, R., Smith, R.K., 1970. Distribution of planktonic foraminifera in the vicinity of the North Atlantic current. Smithson. Contrib. Paleobiol. 4, 1–52.

Conover, W.J., 1980. Practical Nonparametric Statistics. John Wiley & Sons, Ltd., New York.

Coxall, H.K., Wilson, P.A., Pearson, P.N., Sexton, P.F., 2007. Iterative evolution of digitate planktonic foraminifera. Paleobiology 33, 495–516.

Cushman, J.A., 1927. Recent Foraminifera off the west coast of America. Bull. Scripps Inst. Oceanogr. Tech. Ser. 1, 119–188.

d'Orbigny, A., 1839. Foraminifèrs. In: de la Sagra, R. (Ed.), Histoire Physique et Naturelle de L'ile de Cuba. Bertrand A, Paris, p. 82.

Darling, K.F., Wade, C.M., 2008. The genetic diversity of planktic foraminifera and the global distribution of ribosomal RNA genotypes. Mar. Micropaleontol. 67, 216–238.

Darling, K., Wade, C.M., Kroon, D., Leigh Brown, A.J., Bijma, J., 1999. The diversity and distribution of modern planktic foraminiferal small subunit RNA genotypes and their potential as tracers of present and past ocean circulations. Paleoceanography 14, 3–12.

Darling, K.F., Kucera, M., Kroon, D., Wade, C.M., 2006. A resolution for the coiling direction paradox in *Neogloboquadrina pachyderma*. Paleoceanography 21, PA2011.

Darling, K.F., Kucera, M., Wade, C.M., 2007. Global molecular phylogeography reveals persistent Arctic circumpolar isolation in a marine planktonic protist. Proc. Natl. Acad. Sci. U. S. A. 104, 5002–5007.

de Vargas, C., Norris, R., Zaninetti, L., Gibb, S.W., Pawlowski, J., 1999. Molecular evidence of cryptic speciation in planktonic foraminifers and their relation to oceanic provinces. Proc. Natl. Acad. Sci. U. S. A. 96, 2864–2868.

de Vargas, C., Renaud, S., Hilbrecht, H., Pawlowski, J., 2001. Pleistocene adaptive radiation in *Globorotalia truncatulinoides*: genetic, morphologic, and environmental evidence. Paleobiology 27, 104–125.

de Vargas, C., Bonzon, M., Rees, N.W., Pawlowski, J., Zaninetti, L., 2002. A molecular approach to biodiversity and biogeography in the planktonic foraminifer *Globigerinella siphonifera* (d'Orbigny). Mar. Micropaleontol. 45, 101–116.

Development Core Team, R., 2011. R: A Language and Environment for Statistical Computing. R Foundation for Statistical Computing, Vienna.

Drooger, C.W., Kaasschieter, J.P.H., 1958. Foraminifera of the Orinoco–Trinidad–Paria shelf. Verhandelingen der Koninklijke Nederlandse Akademie van Wetenschappen, Afd. Natuurkunde 22, 1–107.

Egger, J.G., 1857. Die foraminiferen der Miocän-Schichten bei Ortenburg in Nieder-Bayern. Neues Jahrbuch der Mineralogie Geognostik Geologie und Petrefakten-Kunde, Stuttgart.

Egger, J.G., 1893. Foraminiferen aus Meeresgrundproben, gelothet von 1874 bis 1876. Verlag der königlichen Akademie, Munich.

Faber, W.W., Anderson, O.R., Lindsey, J.L., Caron, D.A., 1988. Algal–foraminiferal symbiosis in the planktonic foraminifer *Globigerinella aequilateralia*; I. Occurrence and stability of two mutually exclusive chrysophyte endosymbionts and their ultrastructure. J. Foraminifer. Res. 18, 334–343.

Faber, W.W., Anderson, O.R., Caron, D.A., 1989. Algal–foraminiferal symbiosis in the planktonic foraminifer *Globigerinella aequilateralis*; II. Effects of two symbiont species on foraminiferal growth and longevity. J. Foraminifer. Res. 19, 185–193.

Feldman, G.C., McClain, C.R., 2013. Ocean Color Web, AquaMODIS Reprocessing 2012.0. NASA Goddard Space Flight Center.

Felsenstein, J., 1985. Confidence limits on phylogenies: an approach using the Bootstrap. Evolution 39, 783–791.

Fisher, R.A., 1936. The use of multiple measurements in taxonomic problems. Ann. Hum. Genet. 7, 179–188.

Göker, M., Grimm, G.W., Auch, A.F., Aurahs, R., Kucera, M., 2010. A clustering optimization strategy for molecular taxonomy applied to planktonic foraminifera SSU rDNA. Evol. Bioinforma. 6, 97–112.

Helsel, D.R., Hirsch, R.M., 2002. Statistical methods in water resources. Hydrologic Analysis and Interpretation. U.S. Geological Survey, pp. 1–510.

Hemleben, C., Spindler, M., Anderson, O.R., 1989. Modern Planktonic Foraminifera. Springer, Heidelberg.

Hotelling, H., 1933. Analysis of a complex of statistical variables into principal components. J. Educ. Psychol. 24, 417–441.

Huber, B.T., Bijma, J., Darling, K.F., 1997. Cryptic speciation in the living planktonic foraminifer *Globigerinella siphonifera* (d' Orbigny). Paleobiology 23, 33–62.

Katoh, K., Standley, D.M., 2013. MAFFT multiple sequence alignment software version 7: improvements in performance and usability. Mol. Biol. Evol. 30, 772–780.

Kendall, M.G., 1938. A new measurement of rank correlation. Biometrika 30, 81–93.

Kennett, J.P., Srinivasan, M.S., 1983. Neogene Planktonic Foraminifera: A Phylogenetic Atlas. Hutchinson Ross Publishing Co., Stroudsburg, PA.

Kucera, M., Participants, Cruise, 2013. Cruise report of RV Sonne Cruise SO226-3 DipFIP — the extent and structure of cryptic diversity in morphospecies of planktonic Foraminifera of the Indopacific Warm Pool, Wellington–Kaohsiung, 04.03.2013–28.03.2013. Berichte, MARUM — Zentrum für Marine Umweltwissenschaften, Fachbereich Geowissenschaften. Universität Bremen, Bremen.

Kucera, M., Weinelt, M., Kiefer, T., Pflaumann, U., Hayes, A., Weinelt, M., Chen, M.-T., Mix, A.C., Barrows, T.T., Cortijo, E., Duprat, J., Juggins, S., Waelbroeck, C., 2005. Reconstruction of sea-surface temperatures from assemblages of planktonic foraminifera: multi-technique approach based on geographically constrained calibration data sets and its application to glacial Atlantic and Pacific Oceans. Quat. Sci. Rev. 24, 951–998.

Locarnini, R.A., Mishonov, A.V., Antonov, J.I., Boyer, T.P., Garcia, H.E., Baranova, O.K., Zweng, M.M., Paver, C.R., Reagan, J.R., Johnson, D.R., Hamilton, M., Seidov, D., 2013. World Ocean Atlas 2013. In: Levitus, S., Mishonov, A. (Eds.), Temperature Volume 1. NOAA Atlas NESDIS.

Mann, H.B., Whitney, D.R., 1947. On a test of whether one of two random variables is stochastically larger than the other. Ann. Math. Stat. 18, 50–60.

Miller, M.A., Pfeiffer, W., Schwartz, T., 2010. Creating the CIPRES Science Gateway for inference of large phylogenetic trees. Proceedings of the Gateway Computing Environments Workshop (GCE), New Orleans, LA, pp. 1–8.

Morard, R., Quillévéré, F., Escarguel, G., Ujiie, Y., de Garidel-Thoron, T., Norris, R.D., de Vargas, C., 2009. Morphological recognition of cryptic species in the planktonic foraminifer *Orbulina universa*. Mar. Micropaleontol. 71, 148–165.

Morard, R., Quillévéré, F., Douady, C.J., de Vargas, C., de Garidel-Thoron, T., Escarguel, G., 2011. Worldwide genotyping in the planktonic foraminifer *Globoconella inflata*: implications for life history and paleoceanography. PLoS ONE 6, e26665.

Norris, R.D., 1991a. Parallel evolution in the keel structure of planktonic foraminifera. J. Foraminifer. Res. 21, 319–331.

Norris, R.D., 1991b. Biased extinction and evolutionary trends. Paleobiology 17, 388–399.

Parker, F.L., 1958. Eastern Mediterranean foraminifera. Sediment Cores from the Mediterranean Sea and the Red SeaReports on the Swedish Deep Sea Expedition. Elander, Goteborg, pp. 217–283.

Parker, F.L., 1962. Planktonic foraminiferal species in pacific sediments. Micropaleontology 8, 219–254.

Quillévéré, F., Morard, R., Escarguel, G., Douady, C.J., Ujiié, Y., de Garidel-Thoron, T., de Vargas, C., 2013. Global scale same-specimen morpho-genetic analysis of *Truncorotalia truncatulinoides*: A perspective on the morphological species concept in planktonic foraminifera. Palaeogeography, Palaeoclimatology, Palaeoecology 391 Part A: 2-12.

Rhumbler, L., 1909. Die Foraminiferen (Thalamophoren) der Plankton-Expedition. Verlag von Lipsius und Tischer, Kiel and Leipzig.

Saito, T., Thompson, P.R., Breger, D., 1976. Skeletal ultramicrostructure of some elongate-chambered planktonic foraminifera and related species. In: Takayanagi, Y., Saito, T. (Eds.), Progress in Micropaleontology. Micropaleontology Press, American Museum Natural History, New York.

Saito, T., Thompson, P.R., Breger, D., 1981. Systematic Index of Recent and Pleistocene Planktonic Foraminifera. University of Tokyo Press, Tokyo.

Scheirer, J., Ray, W.S., Hare, N., 1976. The analysis of ranked data derived from completely randomized factorial designs. Biometrics 32, 429–434.

Schindelin, J., Arganda-Carreras, I., Frise, E., Kayning, V., Longair, M., Pietzsch, T., Preibisch, S., Rueden, C., Saalfeld, S., Schmid, B., Tinevez, J.-Y., White, D.J., Hartenstein, V., Eliceiri, K., Tomancak, P., Cardona, A., 2012. Fiji: an open-source platform for biological-image analysis. Nat. Methods 9, 676–682.

Schlitzer, R., 2011. Ocean Data View. http://odv.awi.de.

Seears, H., Darling, K., Wade, C., 2012. Ecological partitioning and diversity in tropical planktonic foraminifera. BMC Evol. Biol. 12, 54.

Sen, P.K., 1968. Estimates of the regression coefficient based on Kendall's Tau. J. Am. Stat. Assoc. 63, 1379–1389.

Siccha, M., Trommer, G., Schulz, H., Hemleben, C., Kucera, M., 2009. Factors controlling the distribution of planktonic foraminifera in the Red Sea and implications for the development of transfer functions. Mar. Micropaleontol. 72, 146–156.

Stamatakis, A., 2006. Phylogenetic models of rate heterogeneity: a high performance computing perspective. Parallel and Distributed Processing Symposium. IPDPS, Rhodos, Greece.

Stamatakis, A., Hoover, P., Rougemont, J., 2008. A rapid bootstrap algorithm for the RAxML web servers. Syst. Biol. 57, 758–771.

Theil, H., 1950. A rank-invariant method of linear and polynomial regression analysis, III. Proceedings of the Koninklijke Nederlandse Akademie van Wetenschappen 53, pp. 1397–1412.

Venables, W.N., Ripley, B.D., 2002. Modern Applied Statistics with S, 4th ed. Springer-Verlag.

Walker, D.A., Vilks, G., 1973. Spinal ultrastructure of the planktonic foraminifers *Hastigerina* THOMSON and *Globigerinella* CUSHMAN. J. Foraminifer. Res. 3, 196–198.

Weiner, A., Aurahs, R., Kurasawa, A., Kitazato, H., Kucera, M., 2012. Vertical niche partitioning between cryptic sibling species of a cosmopolitan marine planktonic protist. Mol. Ecol. 21, 4063–4073.

Weiner, A.K.M., Weinkauf, M.F.G., Kurasawa, A., Darling, K.F., Kucera, M., Grimm, G.W., 2014. Phylogeography of the tropical planktonic foraminifera lineage *Globigerinella* reveals isolation inconsistent with passive dispersal by ocean currents. PLoS ONE 9, e92148.